

# Dark Sector Assisted Low Scale Leptogenesis from Three Body Decay without Loops

Debasish Borah,<sup>1,\*</sup> Arnab Dasgupta,<sup>2,†</sup> and Devabrat Mahanta<sup>1,‡</sup>

<sup>1</sup>*Department of Physics, Indian Institute of Technology Guwahati, Assam 781039, India*

<sup>2</sup>*Institute of Convergence Fundamental Studies , Seoul-Tech, Seoul 139-743, Korea*

## Abstract

We study the possibility of realising tree level leptogenesis from three body decay, dark matter and neutrino mass in a minimal framework. We propose a first of its kind model to implement the idea of leptogenesis from three body decay where CP asymmetry arises from interference of multiple tree level diagrams. The standard model is extended by three heavy singlet fermions, one scalar singlet and one scalar doublet with appropriate discrete charges. Two of these singlet fermions not only play non-trivial roles in generating light neutrino mass at radiative level in scotogenic fashion, but also act as mediators in three body decay of the third singlet fermion leading to desired CP asymmetry through interference of tree level diagrams. With just one additional field compared to the minimal scotogenic model, we show that successful leptogenesis can occur at a scale as low as 1 TeV which is lower than the leptogenesis scale found for scotogenic model. Also, the realisation of this tree level three body decay leptogenesis naturally leads to a two component scalar singlet-doublet dark matter scenario offering a rich phenomenology. Apart from having interesting interplay of different couplings involved in processes related to both leptogenesis and dark matter, the model can also be tested at different experiments due to the existence of its particle spectrum at TeV scale.

---

\* [dborah@iitg.ac.in](mailto:dborah@iitg.ac.in)

† [arnabdasgupta@protonmail.ch](mailto:arnabdasgupta@protonmail.ch)

‡ [devab176121007@iitg.ac.in](mailto:devab176121007@iitg.ac.in)

## I. INTRODUCTION

The observed asymmetry between matter and antimatter in the present universe has been a longstanding puzzle in particle physics and cosmology. The excess of baryon over antibaryons is so huge that almost all the visible matter in the universe is in the form of baryons only. It is often quantified in terms of baryon to photon ratio, which, according to Planck 2018 data [1, 2] is

$$\eta_B = \frac{n_B - n_{\bar{B}}}{n_\gamma} = 6.1 \times 10^{-10}. \quad (1)$$

This excess derived from the measurements of cosmic microwave background (CMB) anisotropies matches very well with the predictions of big bang nucleosynthesis (BBN). The observed excess gives rise to a puzzle because we expect the universe to be started in a baryon symmetric manner. Even if we start with an initial asymmetry, the cosmic inflationary phase will make it negligible in latter epochs of the universe. A baryon symmetric universe can evolve into an asymmetric one dynamically if certain conditions, known as Sakharov's conditions [3] are satisfied. They are namely, (1) baryon number (B) violation, (2) C and CP violation and (3) departure from thermal equilibrium. While all these criteria can be satisfied, in principle, in the standard model (SM) of particle physics and an expanding Friedmann-Lemaitre-Robertson-Walker (FLRW) universe, it falls way short of the required amount to produce the huge asymmetry. This has led to different beyond standard model (BSM) proposals out of which the most popular scenario is to consider the existence of some heavy particles whose out-of-equilibrium and B, C, CP violating decays can produce the baryon asymmetry of the universe (BAU) [4, 5]. Instead of generating baryon asymmetry directly, one can generate an asymmetry in the leptonic sector first through similar lepton number (L) violating decays which can later be converted into the observed baryon asymmetry through  $(B + L)$ -violating EW sphaleron transitions [6]. First proposed by Fukugita and Yanagida more than thirty years back [7], this alternate way has come to be known as leptogenesis, a review of which can be found in [8]. An interesting feature of this scenario is that the required lepton asymmetry can be generated through CP violating out-of-equilibrium decays of the same heavy fields that take part in the seesaw mechanism [9–14] that explains the origin of tiny neutrino masses [1], another observed phenomenon the SM fails to address.

While the asymmetric nature of visible matter has been a longstanding puzzle, another

feature of the overall matter component of the present universe adds more to this puzzle. It turns out that only approximately 20% of the present universe's matter density is composed of baryons or visible matter while the rest comes from a mysterious, non-luminous, non-baryonic form of matter, popularly known as dark matter (DM). This is strongly supported by both astrophysical and cosmological observations [1, 2, 15–17]. Similar to the baryon asymmetry, DM abundance is also quantified in terms of a dimensionless quantity as [2]:  $\Omega_{\text{DM}}h^2 = 0.120 \pm 0.001$  at 68% confidence level (CL). Here  $\Omega_{\text{DM}} = \rho_{\text{DM}}/\rho_{\text{critical}}$  is the density parameter of DM and  $h = \text{Hubble Parameter}/(100 \text{ km s}^{-1}\text{Mpc}^{-1})$  is a dimensionless parameter of order unity.  $\rho_{\text{critical}} = 3H^2/(8\pi G)$  is the critical density while  $H$  is the Hubble parameter. Since none of the SM particles can satisfy the criteria for being a DM candidate, several BSM proposals have been put forward out of which the weakly interacting massive particle (WIMP) is the most widely studied one [18, 19]. In the WIMP framework, a DM particle having mass around the electroweak scale and interactions similar to the weak interactions gets thermally produced in the early universe, followed by its decoupling from the thermal bath leading to a freeze-out abundance remarkably close to the observed DM abundance. This coincidence is often referred to as the *WIMP Miracle*.

Motivated by the above two phenomena and neutrino mass which SM fails to explain, we consider a scenario where all three phenomena can be explained in a unified manner. One popular scenario, which can accommodate all these three phenomena is the scotogenic framework proposed by Ma in 2006 [20]. In the minimal version of this framework, the SM is extended by two or three copies of  $Z_2$  odd fermions singlet under SM gauge symmetries, and an additional scalar field similar to the Higgs doublet of the SM, but odd under the unbroken  $Z_2$  symmetry. The salient feature of this framework is the way it connects the origin of light neutrino masses and DM. The unbroken  $Z_2$  symmetry leads to a stable DM candidate while the  $Z_2$  odd particles generate light neutrino masses at one loop level. Apart from this, the out-of-equilibrium decay of the heavy singlet fermions can also lead to successful leptogenesis at a scale as low as 10 TeV. Such low scale leptogenesis with hierarchical right handed neutrinos has been discussed by several authors [21–28] while quasi-degenerate right handed neutrino scenario was discussed in earlier works [29, 30]. For hierarchical right handed neutrinos, such a low scale leptogenesis is a significant improvement over the usual Davidson-Ibarra bound  $M_1 > 10^9 \text{ GeV}$  for vanilla leptogenesis in type I seesaw framework [31].

In this work, we consider the possibility of lowering the scale of leptogenesis further (compared to the ones obtained in previous works) via tree level decay heavy singlet fermions into three different particles including one SM lepton. While leptogenesis from three body decay was covered in earlier works [32–35], leptogenesis from tree level processes was also discussed in different contexts by the authors of [36–40]. However, as far as we are aware of, a concrete model to incorporate tree level leptogenesis from three body decay has not been proposed till now. Here we try to implement the idea of tree level three body decay in a minimal extension of the scotogenic model to achieve successful leptogenesis at a lower scale. Such an extension is required as in the minimal scotogenic model we can not have non-zero CP asymmetry from tree level three body decay. We show that successful leptogenesis can be achieved at a scale as low as 1 TeV in this scenario. While building such a setup, we also find that the model naturally predicts a two component dark matter scenario. We discuss interplay of different couplings involved in leptogenesis as well dark matter and show the consistency between the possibility of low scale leptogenesis and correct DM relic density in agreement with all experimental constraints including light neutrino masses and mixing.

This paper is organised as follows. In section II, we discuss our model in details followed by discussion of leptogenesis and dark matter in section III and IV respectively. We discuss our results in section V and conclude in section VI.

## II. THE MODEL

We briefly discuss our model in this section. We stick to a minimal setup required to obtain the desired phenomenology. The SM particle content is extended by three singlet chiral fermions  $N_{1,2}, \psi$  and two scalar fields  $\eta, S$  which transform non-trivially under the additional  $Z_2 \times Z'_2$  symmetry of the model. This additional discrete symmetry is chosen to remove the unwanted terms so that the desired leptogenesis and dark matter phenomenology can be ensured. UV completion of our model can explain the origin of such discrete gauge symmetries from spontaneous breaking of gauge symmetries at high energy scale, for example see [41–46] and references therein. As we discuss in details below, with the addition of one extra field compared to the minimal scotogenic model [20], we can achieve much richer phenomenology with a new way of generating lepton asymmetry at a scale, lower compared to the one obtained in minimal scotogenic model [24–28].

Particles	$SU(3)_c \times SU(2)_L \times U(1)_Y$	$Z_2$	$Z'_2$
$Q_L$	$(3, 2, \frac{1}{6})$	1	1
$u_R$	$(3, 1, \frac{2}{3})$	1	1
$d_R$	$(3, 1, -\frac{1}{3})$	1	1
$\ell_L$	$(1, 2, -\frac{1}{2})$	1	1
$\ell_R$	$(1, 1, -1)$	1	1
$N_{1,2}$	$(1, 1, 0)$	-1	1
$\psi$	$(1, 1, 0)$	-1	-1
$H$	$(1, 2, \frac{1}{2})$	1	1
$\eta$	$(1, 2, \frac{1}{2})$	-1	1
$S$	$(1, 1, 0)$	1	-1

TABLE I. Particle content of the model.

The particle content of the model is shown in Table I along with their transformations under the symmetries of the model. The Yukawa Lagrangian can be written as

$$\mathcal{L} = -Y_u \overline{Q}_L \tilde{H} u_R - Y_d \overline{Q}_L H d_R - Y_e \overline{\ell}_L H \ell_R - h_{ij} (\overline{\ell}_L)_i \tilde{\eta} N_j - \frac{1}{2} M_j \overline{N}_j^c N_j - y_j \psi N_j S - \frac{1}{2} m_\psi \overline{\psi^c} \psi \quad (2)$$

The scalar potential is given by

$$V = \mu_H^2 H^\dagger H + \mu_\eta^2 \eta^\dagger \eta + \frac{1}{2} m^2 S^2 + \frac{\lambda_1}{2} (H^\dagger H)^2 + \frac{\lambda_2}{2} (\eta^\dagger \eta)^2 + \frac{1}{2} \lambda_S S^4 + \lambda_3 (H^\dagger H) (\eta^\dagger \eta) + \lambda_4 (H^\dagger \eta) (\eta^\dagger H) + \frac{\lambda_5}{2} [(H^\dagger \eta) (H^\dagger \eta) + (\eta^\dagger H) (\eta^\dagger H)] + \frac{\lambda_6}{2} (H^\dagger H) S^2 + \lambda_7 (\eta^\dagger \eta) S^2. \quad (3)$$

After the electroweak symmetry breaking (EWSB), the two scalar doublets of the model can be written in the following form in the unitary gauge:

$$H = \begin{pmatrix} 0 \\ \frac{v+h}{\sqrt{2}} \end{pmatrix}, \quad \eta = \begin{pmatrix} \eta^\pm \\ \frac{\eta_R + i\eta_I}{\sqrt{2}} \end{pmatrix}, \quad (4)$$

where  $h$  is the SM-like Higgs boson,  $\eta_R$ ,  $\eta_I$  are the CP-even and CP-odd neutral scalars respectively, while  $\eta^\pm$  are the charged scalars from the additional scalar doublet  $\eta$ . The vacuum expectation value (VEV) of the SM Higgs is denoted by  $v$  while the other two scalars do not acquire any VEVs so that the  $Z_2 \times Z'_2$  symmetry of the model remains unbroken.

The masses of the physical scalars at tree level can be written as

$$\begin{aligned}
m_h^2 &= \lambda_1 v^2, \quad m_S^2 = m^2 + \lambda_6 \frac{v^2}{2}, \quad m_{\eta^\pm}^2 = \mu_\eta^2 + \frac{1}{2} \lambda_3 v^2 \\
m_{\eta_R}^2 &= \mu_\eta^2 + \frac{1}{2} (\lambda_3 + \lambda_4 + \lambda_5) v^2 = m_{\eta^\pm}^2 + \frac{1}{2} (\lambda_4 + \lambda_5) v^2, \\
m_{\eta_I}^2 &= \mu_\eta^2 + \frac{1}{2} (\lambda_3 + \lambda_4 - \lambda_5) v^2 = m_{\eta^\pm}^2 + \frac{1}{2} (\lambda_4 - \lambda_5) v^2.
\end{aligned} \tag{5}$$

Without any loss of generality, we consider  $\lambda_5 < 0$  so that the CP-even scalar is lighter than the CP-odd one. Thus  $\eta_R$  is the lightest component of the scalar doublet  $\eta$  and also lighter than the singlet fermions  $N_{1,2}$ . Similarly the singlet scalar  $S$  is chosen to be lighter than  $\psi$ . This ensures  $\eta_R, S$  to be the lightest  $Z_2$ -odd and  $Z'_2$ -odd particles respectively and hence viable dark matter candidates of the model.

As can be seen from the Yukawa Lagrangian in equation (2), there is no tree level contribution to light neutrino masses, simply because they couple to the heavy neutrinos  $N_i$  only via the second scalar doublet  $\eta$  which does not acquire any VEV. However, light neutrino masses can arise at radiative level as originally proposed in the context of minimal scotogenic model [20]. In our setup, the additional scalar doublet  $\eta$  and the singlet fermions  $N_{1,2}$  will go inside the loop which generates the light neutrino masses, the expression for which can be evaluated as [20, 47]

$$\begin{aligned}
(M_\nu)_{ij} &= \sum_k \frac{h_{ik} h_{jk} M_k}{32\pi^2} \left( \frac{m_{\eta_R}^2}{m_{\eta_R}^2 - M_k^2} \ln \frac{m_{\eta_R}^2}{M_k^2} - \frac{m_{\eta_I}^2}{m_{\eta_I}^2 - M_k^2} \ln \frac{m_{\eta_I}^2}{M_k^2} \right) \\
&\equiv \sum_k \frac{h_{ik} h_{jk} M_k}{32\pi^2} [L_k(m_{\eta_R}^2) - L_k(m_{\eta_I}^2)],
\end{aligned} \tag{6}$$

where  $M_k$  is the mass eigenvalue of the mass eigenstate  $N_k$  in the internal line and the indices  $i, j = 1, 2, 3$  run over the three neutrino generations and  $k = 1, 2$  takes into account of two  $N_i$ . The loop function  $L_k(m^2)$  is defined as

$$L_k(m^2) = \frac{m^2}{m^2 - M_k^2} \ln \frac{m^2}{M_k^2}. \tag{7}$$

From the expressions for physical scalar masses given in equations (5), we can write  $m_{\eta_R}^2 - m_{\eta_I}^2 = \lambda_5 v^2$ . Therefore, in the limit  $\lambda_5 \rightarrow 0$ , the neutral components of inert doublet  $\eta$  become mass degenerate. Also, a vanishing  $\lambda_5$  implies vanishing light neutrino masses which is expected as the  $\lambda_5$ -term in the scalar potential (3) breaks lepton number by two units, when considered together with the fermion Yukawa Lagrangian (2). As we will see

later, this parameter also plays crucial role in both leptogenesis and DM phenomenology. It should also be noted that the Yukawa coupling  $h_{ik}$  is a  $3 \times 2$  matrix in flavour basis due to the existence of only two right handed neutrinos appearing in light neutrino mass. This predicts a vanishing lightest neutrino mass.

In order to ensure that the choice of Yukawa couplings as well as other parameters involved in light neutrino mass formula discussed above are consistent with the cosmological upper bound on the sum of neutrino masses,  $\sum_i m_i \leq 0.11$  eV [2], as well as the neutrino oscillation data [48, 49], it is often useful to rewrite the neutrino mass formula given in equation (6) in a form similar to the well known the type-I seesaw formula:

$$M_\nu = h\Lambda^{-1}h^T, \quad (8)$$

where we have introduced the diagonal matrix  $\Lambda$  with elements

$$\Lambda_i = \frac{2\pi^2}{\lambda_5} \zeta_i \frac{2M_i}{v^2}, \quad (9)$$

$$\text{and } \zeta_i = \left( \frac{M_i^2}{8(m_{\eta_R}^2 - m_{\eta_I}^2)} [L_i(m_{\eta_R}^2) - L_i(m_{\eta_I}^2)] \right)^{-1}. \quad (10)$$

The light neutrino mass matrix (8) which is complex symmetric by virtue of Majorana nature, can be diagonalised by the usual Pontecorvo-Maki-Nakagawa-Sakata (PMNS) mixing matrix  $U$  (in the diagonal charged lepton basis), written in terms of neutrino oscillation data (up to the Majorana phases) as

$$U = \begin{pmatrix} c_{12}c_{13} & s_{12}c_{13} & s_{13}e^{-i\delta} \\ -s_{12}c_{23} - c_{12}s_{23}s_{13}e^{i\delta} & c_{12}c_{23} - s_{12}s_{23}s_{13}e^{i\delta} & s_{23}c_{13} \\ s_{12}s_{23} - c_{12}c_{23}s_{13}e^{i\delta} & -c_{12}s_{23} - s_{12}c_{23}s_{13}e^{i\delta} & c_{23}c_{13} \end{pmatrix} U_{\text{Maj}} \quad (11)$$

where  $c_{ij} = \cos \theta_{ij}$ ,  $s_{ij} = \sin \theta_{ij}$  and  $\delta$  is the leptonic Dirac CP phase. The diagonal matrix  $U_{\text{Maj}} = \text{diag}(1, e^{i\alpha}, e^{i(\zeta+\delta)})$  contains the undetermined Majorana CP phases  $\alpha, \zeta$ . The diagonal light neutrino mass matrix is therefore,

$$D_\nu = U^\dagger M_\nu U^* = \text{diag}(m_1, m_2, m_3). \quad (12)$$

where the light neutrino masses can follow either normal ordering (NO) or inverted ordering (IO). As mentioned earlier, the model predicts a vanishing lightest neutrino mass implying  $m_1 = 0$  (NO) and  $m_3 = 0$  (IO). Since the inputs from neutrino oscillation data are only in

terms of the two mass squared differences and three mixing angles, it would be useful for our purpose to express the Yukawa couplings ( $h$ ) in terms of light neutrino parameters. This is possible through the Casas-Ibarra (CI) parametrisation [50] extended to radiative seesaw model [51] which allows us to write the Yukawa coupling matrix satisfying the neutrino data as

$$h_{ij} = (UD_\nu^{1/2}R^\dagger\Lambda^{1/2})_{ij}, \quad (13)$$

where  $R$  is an arbitrary complex orthogonal matrix satisfying  $RR^T = \mathbb{1}$ . It is worth mentioning that, since we have only two right handed neutrinos  $N_{1,2}$  taking part in generating radiative light neutrino masses, the lightest neutrino mass is vanishing. Also, in case of only two right handed neutrinos, the  $R$  matrix is a function of only one complex rotation parameter  $z = z_R + iz_I, z_R \in [0, 2\pi], z_I \in \mathbb{R}$  [52] which can affect the results of leptogenesis as we discuss below.

### A. Constraints on Model Parameters

Precision measurements at LEP experiment forbids additional decay channels of the SM gauge bosons. For example, it strongly constrains the decay channel  $Z \rightarrow \eta_R\eta_I$  requiring  $m_{\eta_R} + m_{\eta_I} > m_Z$ . Additionally, LEP precision data also rule out the region  $m_{\eta_R} < 80$  GeV,  $m_{\eta_I} < 100$  GeV,  $m_{\eta_I} - m_{\eta_R} > 8$  GeV [53]. We take the lower bound on charged scalar mass  $m_{\eta^\pm} > 90$  GeV. If  $m_{\eta_R, \eta_I} < m_h/2$ , the large hadron collider (LHC) bound on invisible Higgs decay comes into play. The constraint on the Higgs invisible decay branching fraction from the ATLAS experiment at LHC is [54]

$$\mathcal{B}(h \rightarrow \text{Invisible}) = \frac{\Gamma(h \rightarrow \text{Invisible})}{\Gamma(h \rightarrow SM) + \Gamma(h \rightarrow \text{Invisible})} \leq 26\% \quad (14)$$

while the recent ATLAS announcement [55] puts a more stringent constraint at 13%. This can constrain the SM Higgs coupling with  $\eta_R, \eta_I, S$  namely  $\lambda_3 + \lambda_4 \pm \lambda_5, \lambda_6$  respectively to be smaller than around  $10^{-3}$  in the regime  $m_{\eta_R}, m_{\eta_I}, m_S < m_h/2$  which however remains weaker than DM direct detection bounds in this mass regime (see for example, [56]).

Additionally, the LHC experiment can also put bounds on the scalar masses in the model, specially the components of scalar doublet  $\eta$  as they can be pair produced copiously in proton proton collisions leading to different final states which are being searched for. Depending



upon the mass spectrum of its components, the heavier ones can decay into the lighter ones and a gauge boson, which finally decays into a pair of leptons or quarks. Therefore, we can have either pure leptonic final states plus missing transverse energy (MET), hadronic final states plus MET or a mixture of both. The MET corresponds to DM or light neutrinos. In several earlier works [57–59], the possibility of opposite sign dileptons plus MET was discussed. In [60], the possibility of dijet plus MET was investigated with the finding that inert scalar masses up to 400 GeV can be probed at high luminosity LHC. In another work [61], tri-lepton plus MET final states was also discussed whereas mono-jet signatures have been studied by the authors of [62, 63]. The enhancement in dilepton plus MET signal in the presence of additional vector like singlet charged leptons was also discussed in [64]. Exotic signatures like displaced vertex and disappearing or long-lived charged track for compressed mass spectrum of inert scalars and singlet fermion DM was studied recently by the authors of [65].

In addition to the collider or direct search constraints, there exists theoretical constraints also. For instance, the scalar potential of the model should be bounded from below in any field direction. This criteria leads to the following co-positivity conditions [66–68]:

$$\begin{aligned}
&\lambda_{1,2,S} \geq 0, \quad \lambda_3 + \sqrt{\lambda_1 \lambda_2} \geq 0, \\
&\lambda_3 + \lambda_4 - |\lambda_3| + \sqrt{\lambda_1 \lambda_2} \geq 0, \quad \lambda_6 + 2\sqrt{\lambda_1 \lambda_S} \geq 0, \\
&\sqrt{\lambda_1 \lambda_2 \lambda_S} + 2(\lambda_3 \sqrt{\lambda_S} + \lambda_7 \sqrt{\lambda_1} + \frac{\lambda_6}{2} \sqrt{\lambda_2}) \\
&+ 4\sqrt{\frac{1}{2}(\lambda_3 + \frac{1}{2} \sqrt{\lambda_1 \lambda_2})(\lambda_6 + \sqrt{\lambda_1 \lambda_S})(\lambda_7 + \frac{1}{2} \sqrt{\lambda_2 \lambda_6})} \geq 0.
\end{aligned} \tag{15}$$

The coupling constants appeared in above expressions are evaluated at the electroweak scale,  $v$ . Also, in order to avoid perturbative breakdown, all dimensionless couplings like quartic couplings  $(\lambda_i, \lambda_S)$ , Yukawa couplings  $(Y_{ij}, h_{ij}, y_i)$ , gauge couplings  $(g_i)$  should obey the the perturbativity conditions:

$$|\lambda_{1,2,3,4,5,6,7}| < 4\pi, \quad |\lambda_S| < 4\pi, \quad |Y_{u,d,e}, h_{ij}, y_{1,2}| < \sqrt{4\pi}, \quad |g_s, g, g'| < \sqrt{4\pi} \tag{16}$$

### III. LEPTOGENESIS

In this section, we discuss the details of a new way of generating lepton asymmetry at low scale in our model. Note that, similar to the minimal scotogenic model, here also

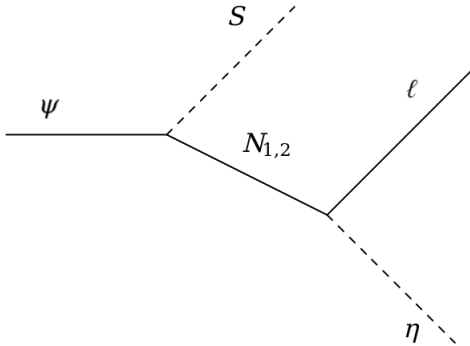


FIG. 1. Three body decay of singlet fermion  $\psi$

there are two different ways of generating lepton asymmetry: out of equilibrium decay of the  $N_i$  [21–30] or annihilation/scattering of dark sector particles [69, 70]. In [21, 22], the authors considered a hierarchical right handed neutrino spectrum to show that successful leptogenesis from two body decay can occur at a scale as low as a few tens of TeV. Leptogenesis with quasi-degenerate right handed neutrinos in scotogenic model was discussed in [29, 30]. In more recent works [24, 25], successful leptogenesis was shown to be possible at a scale as low as 10 TeV even with hierarchical right handed neutrinos while requiring to be in a weak washout regime predicting a vanishingly small lightest neutrino mass. If leptogenesis occurs only from two heavy neutrinos, then the scale of leptogenesis is pushed above the TeV scale by a few order of magnitudes [26]. This will correspond to our scenario if we do not have  $\psi, S$  in our model. To summarise, it has been shown in the above mentioned works that the scale of leptogenesis in scotogenic model can be as low as a few TeV without requiring any resonance enhancement arising due to tiny mass splitting of right handed neutrinos. This significant improvement over the usual Davidson-Ibarra bound on the scale of leptogenesis  $M_N > 10^9$  GeV for vanilla leptogenesis in type I seesaw framework [31] makes the scotogenic model a very attractive and testable framework for leptogenesis. We also note that high scale leptogenesis in scotogenic model was also studied recently by the authors of [71].

In addition to the usual  $1 \rightarrow 2$  decay or  $2 \rightarrow 2$  annihilations as sources of lepton asymmetry, we can also have  $1 \rightarrow 3$  decay in our model. Such three body decay as a source of lepton asymmetry was discussed earlier by several authors [32–35] in the different contexts like radiative seesaw models, R parity violating supersymmetry and so on. Our present work is motivated two features namely, (i) dark matter particles assist in such three body decay

processes and (ii) non-zero lepton asymmetry can be generated due to interference of two tree level decay diagrams without requiring any loop. We show that for our chosen regime of parameter space, such three body decay leptogenesis can be dominant over other possible sources of leptogenesis and the scale of leptogenesis can be lower than what was found by considering two body decay or annihilation processes discussed in earlier works.

In our model, we consider the three body decay of singlet fermion  $\psi$  as the origin of CP asymmetry through the process shown in figure 1<sup>1</sup>. To prevent the two body decay of  $\psi$  into  $N_i, S$  we impose the kinematical constraint  $m_\psi < M_i + m_S$ . The relevant decay processes that can generate Lepton asymmetry are  $\psi \rightarrow Sl\eta$  and  $N_1 \rightarrow \eta l$ . Although  $N_2$  decay can also generate lepton asymmetry in principle, we consider the asymmetry generated by  $N_2$  decay or any pre-existing asymmetry to be negligible due to strong washout effects mediated either by  $N_1$  or  $N_2$  themselves, to be discussed below. The corresponding CP asymmetry parameters are defined as

$$\epsilon_\psi = \frac{\Gamma_{\psi \rightarrow Sl\eta} - \Gamma_{\psi \rightarrow S\bar{l}\eta^*}}{\Gamma_{\psi \rightarrow Sl\eta} + \Gamma_{\psi \rightarrow S\bar{l}\eta^*}}, \quad \epsilon_{N_1} = \frac{\Gamma_{N_1 \rightarrow l\eta} - \Gamma_{N_1 \rightarrow \bar{l}\eta^*}}{\Gamma_{N_1 \rightarrow l\eta} + \Gamma_{N_1 \rightarrow \bar{l}\eta^*}} \quad (17)$$

The details of these CP asymmetry parameters are given in appendix A, B respectively. Along with these two decay processes contributing to the creation of lepton asymmetry, there are washout processes too which tend to destroy the asymmetry created. The relevant washout processes in our model can be categorised as

- Inverse decays:  $l\eta \rightarrow N_1, l\eta S \rightarrow \psi$
- $\Delta L = 1$  scatterings:  $S\ell \rightarrow \psi\eta, l\eta \rightarrow \psi S, \psi\ell \rightarrow S\eta, l\eta \rightarrow N_i(W^\pm, Z)$ .
- $\Delta L = 2$  scatterings:  $l\ell \rightarrow N_i N_i, ll \rightarrow \eta\eta, \eta\ell \rightarrow \eta^*\bar{\ell}$ .

The Boltzmann equations relevant for leptogenesis in this model can be summarised as

$$\frac{dn_\psi}{dz} = -D_\psi(n_\psi - n_\psi^{\text{eq}}) + D_{N_1 \rightarrow \psi S}(n_{N_1} - n_{N_1}^{\text{eq}}) - W_{ID_{N_1 \rightarrow \psi S}}n_\psi - \frac{s}{H(z)z}[(n_\psi n_\eta - n_\psi^{\text{eq}} n_\eta^{\text{eq}})\langle\sigma v\rangle_{\psi\eta \rightarrow Sl} + [n_\psi n_S - n_\psi^{\text{eq}} n_S^{\text{eq}}]\langle\sigma v\rangle_{\psi S \rightarrow l\eta}], \quad (18)$$

$$(19)$$

---

<sup>1</sup> In the absence of this process, the source of leptogenesis will be from decay of  $N_{1,2}$  only and it was shown earlier that in such two right handed neutrino limit of scotogenic model, the scale of leptogenesis is pushed towards higher side [26].

$$\begin{aligned} \frac{dn_{N_1}}{dz} &= -D_{N_1}(n_{N_1} - n_{N_1}^{\text{eq}}) - D_{N_1 \rightarrow \psi S}(n_{N_1} - n_{N_1}^{\text{eq}}) - \frac{s}{H(z)z} [(n_{N_1}^2 - (n_{N_1}^{\text{eq}})^2) \langle \sigma v \rangle_{N_1 N_1 \rightarrow ll} \\ &\quad + [n_{N_1} n_{SM} - n_{N_1}^{\text{eq}} n_{SM}^{\text{eq}}] \langle \sigma v \rangle_{\eta l \rightarrow N_1 (W^\pm, Z)}], \end{aligned} \quad (20)$$

$$(21)$$

$$\begin{aligned} \frac{dn_{B-L}}{dz} &= -\epsilon_\psi D_\psi (n_\psi - n_\psi^{\text{eq}}) - \epsilon_{N_1} D_{N_1} (n_{N_1} - n_{N_1}^{\text{eq}}) - (W_{N_1} + W_\psi) n_{B-L} \\ &\quad - \frac{s}{H(z)z} [\Gamma_{Sl \rightarrow \psi \eta} + \Gamma_{l\eta \rightarrow \psi S} + \Gamma_{ll \rightarrow \eta \eta} + \Gamma_{ll \rightarrow N_1 N_1} + \Gamma_{l\eta \rightarrow (N_1 W^\pm, Z)} + \Gamma_{\eta l \rightarrow \eta^* l}] n_{B-L}. \end{aligned} \quad (22)$$

In the above equations  $z = \frac{m_\psi}{T}$  and  $n_f^{\text{eq}} = \frac{z^2}{2} \kappa_2(z)$  is the equilibrium number density of  $f \equiv N_1, \psi$  (with  $\kappa_i(z)$  being the modified Bessel function of  $i$ -th kind). The quantity  $D_f$  on the right hand side of above equations is

$$\begin{aligned} D_{N_1} &= K_{N_1} z \left( \frac{M_1}{m_\psi} \right) \frac{\kappa_1 \left[ z \left( \frac{M_1}{m_\psi} \right) \right]}{\kappa_2 \left[ z \left( \frac{M_1}{m_\psi} \right) \right]}, \\ D_\psi &= K_\psi z \frac{\kappa_1(z)}{\kappa_2(z)}, \quad D_{N_1 \rightarrow \psi S} = K_{N_1 \rightarrow \psi S} z \left( \frac{M_1}{m_\psi} \right) \frac{\kappa_1 \left[ z \left( \frac{M_1}{m_\psi} \right) \right]}{\kappa_2 \left[ z \left( \frac{M_1}{m_\psi} \right) \right]}. \end{aligned} \quad (23)$$

Here, the decay parameters are defined as

$$K_{N_1} = \frac{\Gamma_{N_1 \rightarrow l\eta}}{H(m_\psi)}, \quad K_\psi = \frac{\Gamma_{\psi \rightarrow Sl\eta}}{H(m_\psi)}, \quad K_{N_1 \rightarrow \psi S} = \frac{\Gamma_{N_1 \rightarrow \psi S}}{H(m_\psi)} \quad (24)$$

with  $\Gamma_f$  is the partial decay width of particle  $f$  for the specified decay process,  $H$  is the Hubble parameter. Since leptogenesis is a high scale phenomena and occurs in the radiation dominated phase of the universe, the Hubble parameter can be expressed in terms of the temperature  $T$  as follows

$$H = \sqrt{\frac{8\pi^3 g_*}{90}} \frac{T^2}{M_{\text{Pl}}} = H(z=1) \frac{1}{z^2} \quad (25)$$

where  $g_*$  is the effective number of relativistic degrees of freedom and  $M_{\text{Pl}} \simeq 1.22 \times 10^{19}$  GeV is the Planck mass. The washout terms are given as

$$\begin{aligned} W_{N_1} &= \frac{1}{4} z^3 \left( \frac{M_1}{m_\psi} \right)^3 \kappa_{N_1} \left[ z \frac{M_1}{m_\psi} \right], \quad W_\psi = \frac{1}{4} z^3 \kappa_\psi(z), \\ W_{N_1 \rightarrow \psi S} &= \frac{1}{4} z^3 \left( \frac{M_1}{m_\psi} \right)^3 \kappa_{N_1 \rightarrow \psi S} \left[ z \frac{M_1}{m_\psi} \right], \end{aligned} \quad (26)$$

The decay process  $N_1 \rightarrow \psi S$  does not contribute to the CP asymmetry but can affect the abundance of  $\psi, N_1$  as can be seen from the Boltzmann equations written above. The decay width for the decay  $N_1 \rightarrow \psi S$  is given by

$$\Gamma_{N_1 \rightarrow \psi S} = \frac{y_1^2}{2\pi} M_1 \sqrt{\left(\frac{m_S^2 - m_\psi^2}{M_1^2}\right)^2 + \left(1 - \frac{2(m_\psi^2 + m_S^2)}{M_1^2}\right)} \left(1 + \frac{\sqrt{4M_1^2 m_S^2 + (m_S^2 - m_\psi^2)^2 + M_1^2(M_1^2 - 2(m_\psi^2 + m_S^2))}}{\sqrt{4M_1^2 m_\psi^2 + (m_S^2 - m_\psi^2)^2 + M_1^2(M_1^2 - 2(m_\psi^2 + m_S^2))}}\right)^{-1} \quad (27)$$

As mentioned earlier, we use the Casas-Ibarra parametrisation to rewrite the Yukawa coupling  $h_{ij}$  in terms of light neutrino parameters. Also, in the case of two right handed neutrinos taking part in generating light neutrino masses in our model, the complex orthogonal matrix  $R$  is a function of only one rotation parameter  $z = z_R + iz_I, z_R \in [0, 2\pi], z_I \in \mathbb{R}$  [50, 52]. Our choice of  $R$  matrix is

$$R = \begin{pmatrix} 0 & \cos(z_R + iz_I) & \sin(z_R + iz_I) \\ 0 & -\sin(z_R + iz_I) & \cos(z_R + iz_I) \end{pmatrix} \quad (28)$$

Then the Yukawa matrix for normal ordering of light neutrino masses can then be explicitly written as

$$h = \begin{pmatrix} \sqrt{m_2}\sqrt{\Lambda_1}\cos(z)U_{12} + \sqrt{m_3}\sqrt{\Lambda_1}\sin(z)U_{13} & -\sqrt{m_2}\sqrt{\Lambda_2}\sin(z)U_{12} + \sqrt{m_3}\sqrt{\Lambda_2}\cos(z)U_{13} \\ \sqrt{m_2}\sqrt{\Lambda_1}\cos(z)U_{22} + \sqrt{m_3}\sqrt{\Lambda_1}\sin(z)U_{23} & -\sqrt{m_2}\sqrt{\Lambda_2}\sin(z)U_{22} + \sqrt{m_3}\sqrt{\Lambda_2}\cos(z)U_{23} \\ \sqrt{m_2}\sqrt{\Lambda_1}\cos(z)U_{32} + \sqrt{m_3}\sqrt{\Lambda_1}\sin(z)U_{33} & -\sqrt{m_2}\sqrt{\Lambda_2}\sin(z)U_{32} + \sqrt{m_3}\sqrt{\Lambda_2}\cos(z)U_{33} \end{pmatrix} \quad (29)$$

with  $U_{ij}$  being the elements of the PMNS mixing matrix mentioned earlier. The other Yukawa coupling which affects lepton asymmetry namely,  $y_i$  is not related to the origin of light neutrino mass and hence we keep it as a free parameter. The choice of this Yukawa coupling affect both leptogenesis and dark matter as we discuss in upcoming sections.

After obtaining the numerical solutions of the above Boltzmann equations (19), (21) and (22), we convert the final  $B-L$  asymmetry  $n_{B-L}^f$  just before electroweak sphaleron freeze-out into the observed baryon to photon ratio by the standard formula

$$\eta_B = \frac{3g_*^0}{4g_*} a_{\text{sph}} n_{B-L}^f \simeq 9.2 \times 10^{-3} n_{B-L}^f, \quad (30)$$

where  $a_{\text{sph}} = \frac{8}{23}$  is the sphaleron conversion factor (taking into account two Higgs doublets). We take the effective relativistic degrees of freedom to be  $g_* = 111.75$ , slightly higher than

that of the SM at such temperatures as we are including the contribution of the inert doublet as well as the scalar singlet too. The heavy singlet fermions  $N_{1,2}, \psi$  do not contribute as they have already decoupled from the bath by this epoch. In the above expression  $g_*^0 = \frac{43}{11}$  is the effective relativistic degrees of freedom at the recombination epoch.

#### IV. DARK MATTER

As mentioned earlier, our model has two DM candidates both of which are stable due to the unbroken  $Z_2 \times Z'_2$  symmetry. Although a two component DM was not part of the original motivation, it emerged naturally due to the chosen charge assignments of different particles namely,  $\eta, S, \psi, N_i$  under  $Z_2 \times Z'_2$  symmetry. In fact, the introduction of the second  $Z_2$  symmetry, necessary to forbid direct coupling of  $\psi$  with SM leptons, has given rise to the second DM component in the model. A very recent study on such two component DM with scalar doublet and scalar singlet can be found in [72]. For some earlier works on multi-component dark matter, please refer to [45, 46, 56, 70, 73–104] and references therein.

Relic abundance of two component DM in our model  $\eta_R, S$  can be found by numerically solving the corresponding Boltzmann equations. Let  $n_1 = n_{\eta_R}$  and  $n_2 = n_S$  are the total number densities of two dark matter candidates respectively. The two coupled Boltzmann equations in terms of  $n_2$  and  $n_1$  are given below [45],

$$\frac{dn_1}{dt} + 3n_1H = -\langle\sigma v_{\eta_R\eta_R\rightarrow X\bar{X}}\rangle (n_1^2 - (n_1^{\text{eq}})^2) - \langle\sigma v_{\eta_R\eta_R\rightarrow SS}\rangle \left( n_1^2 - \frac{(n_1^{\text{eq}})^2}{(n_2^{\text{eq}})^2} n_2^2 \right), \quad (31)$$

$$\frac{dn_2}{dt} + 3n_2H = -\langle\sigma v_{SS\rightarrow X\bar{X}}\rangle (n_2^2 - (n_2^{\text{eq}})^2) + \langle\sigma v_{\eta_R\eta_R\rightarrow SS}\rangle \left( n_1^2 - \frac{(n_1^{\text{eq}})^2}{(n_2^{\text{eq}})^2} n_2^2 \right), \quad (32)$$

where,  $n_i^{\text{eq}}$  is the equilibrium number density of dark matter species  $i$  and  $H$  denotes the Hubble parameter, defined earlier. In the annihilation processes,  $X$  denotes all particles where DM can annihilate into. In the above equations,  $\langle\sigma v\rangle$  is the thermally averaged annihilation cross section, given by [105]

$$\langle\sigma v\rangle_{\text{DMDM}\rightarrow X\bar{X}} = \frac{1}{8m_{\text{DM}}^4 T \kappa_2^2 \left(\frac{m_{\text{DM}}}{T}\right)} \int_{4m_{\text{DM}}^2}^{\infty} \sigma(s - 4m_{\text{DM}}^2) \sqrt{s} \kappa_1 \left(\frac{\sqrt{s}}{T}\right) ds, \quad (33)$$

where  $\kappa_i(x)$ 's are modified Bessel functions of order  $i$  mentioned before. The annihilation processes of scalar singlet scalar doublet are shown in figure IV and IV respectively. While

for scalar singlet DM alone, there is no coannihilation processes, scalar doublet dark matter in scotogenic model can have several coannihilation processes, either with the heavier components of the doublet or fermions as shown in figure IV. Such coannihilation effects within the framework of inert doublet model as well as scotogenic model have already been studied in details by several authors [21, 58, 106–119]. In the presence of coannihilations, one follows the recipe given by [120] to calculate the relic abundance. Since scalar singlet DM has just one component, there is no such coannihilations present. Similar to the inert doublet dark matter model, scalar singlet dark matter has also been studied extensively by several authors [121–125].

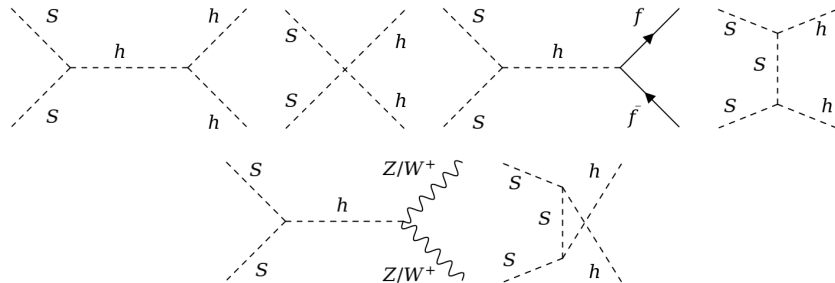


FIG. 2. Feynman diagrams for relevant annihilation processes for singlet scalar DM.

The second terms on the right hand side of the above Boltzmann equations specifically consider the conversions between two DM candidates  $\eta_R, S$  while assuming the former to be the heavier DM component. Such a conversion can occur either directly due to the  $\lambda_6$  coupling of the scalar potential given in equation (3) or via SM Higgs portal interactions. These conversion processes are shown in figure IV. There can be another conversion process due to the interactions shown in the Feynman diagram of figure 1. This can occur due to coannihilation processes, not shown in above Boltzmann equations. In our model, however, singlet scalar DM can, in principle, coannihilate with other particles involved in the same Feynman diagram of figure 1. Since the two DM candidates are stabilised by two separate  $Z_2$  symmetries, their coannihilation can only lead to  $\psi$  which is odd under both the  $Z_2$  symmetries. Alternatively, one of the DM can also coannihilate with  $\psi$  and convert into the other DM. These processes are shown in figure IV. Since we consider  $\psi$  to be heavier than both the DM candidates, we do not show it in the final states.

In order to cover all the features of annihilations, coannihilations as well as conversions,

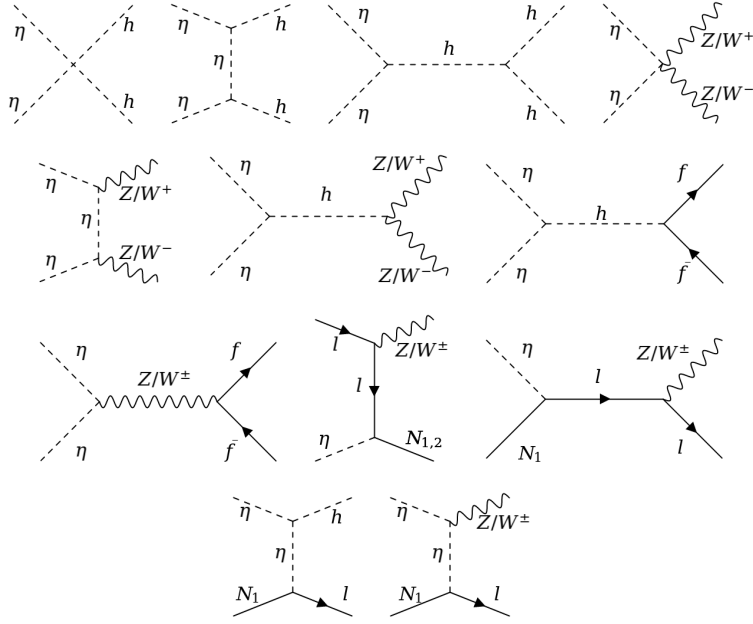


FIG. 3. Feynman diagrams of all the relevant processes for scalar doublet dark matter in scotogenic model. Here DM is chosen to be the real scalar component of the doublet.

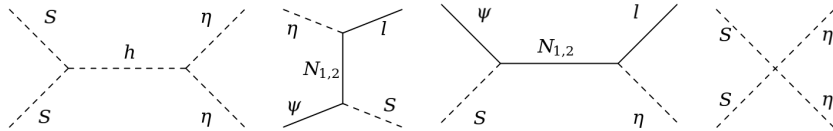


FIG. 4. Feynman diagrams of all the relevant processes determining the DM relic density which emerged due to the extension of the scotogenic model.

we use `micrOMEGAs` [126] to calculate the relic abundance of two component DM in our model. The model information has been supplied to `micrOMEGAs` using `FeynRules` [127] while all the relevant annihilation and coannihilation cross sections of dark matter number changing processes required to solve the coupled equations are calculated using `CalcHEP` [128]. While singlet scalar DM annihilates either through four point scalar interactions or SM Higgs mediated processes, the scalar doublet DM can annihilate (coannihilate) via Higgs as well as electroweak gauge boson portals apart from the four point interactions with Higgs as well as gauge bosons. Additionally, the conversion coupling  $\lambda_6$  as well as Yukawa coupling  $y_i$  can play significant role in individual as well as total DM relic densities.



Just like the SM Higgs boson mediates DM annihilation into SM particles, similarly, it can also mediate spin independent DM-nucleon scatterings. Different ongoing experiments like Xenon1T [129, 130], LUX [131], PandaX-II [132, 133] are trying to detect the DM in the lab-based experiments and give a strong upper bound on the spin-independent (SI) direct detection (DD) cross-section as a function of DM mass. We have extracted the SI elastic scattering cross-section for both the DM candidates from `micrOMEGAs`. DD analysis for two-component DM is slightly different from the single component scenario. To compare the result of our model with Xenon1T bound, we have multiplied the elastic scattering cross-section by the relative number density of each DM candidate and used the following conditions

$$\begin{aligned}\sigma_1^{\text{eff}} &= \frac{n_1}{n_1 + n_2} \sigma_1^{\text{SI}} \leq \sigma_{\text{Xenon1T}} \\ \sigma_2^{\text{eff}} &= \frac{n_2}{n_1 + n_2} \sigma_2^{\text{SI}} \leq \sigma_{\text{Xenon1T}}\end{aligned}\tag{34}$$

Further details related to the direct detection of multi component DM can be found in [134, 135].

## V. RESULTS AND DISCUSSION

In this section, we discuss our numerical results for leptogenesis as well as dark matter separately.

### A. Leptogenesis

To calculate the lepton asymmetry, we first solve the coupled Boltzmann equations (19), (21) and (22) numerically to estimate the final B-L asymmetry. We considered two possible ranges for  $N_1$  mass  $M_1$ . In the first case we have chosen  $N_1$  to be almost degenerate in mass with  $\eta$  and in the second case  $N_1$  mass is significantly higher than  $\eta$  mass. On the other hand  $N_2$  remains heavier than  $N_1$  in both the cases and the mass of  $\psi$  satisfies the relation  $m_\psi < M_i + m_S$  mentioned earlier. We now discuss these two cases separately.

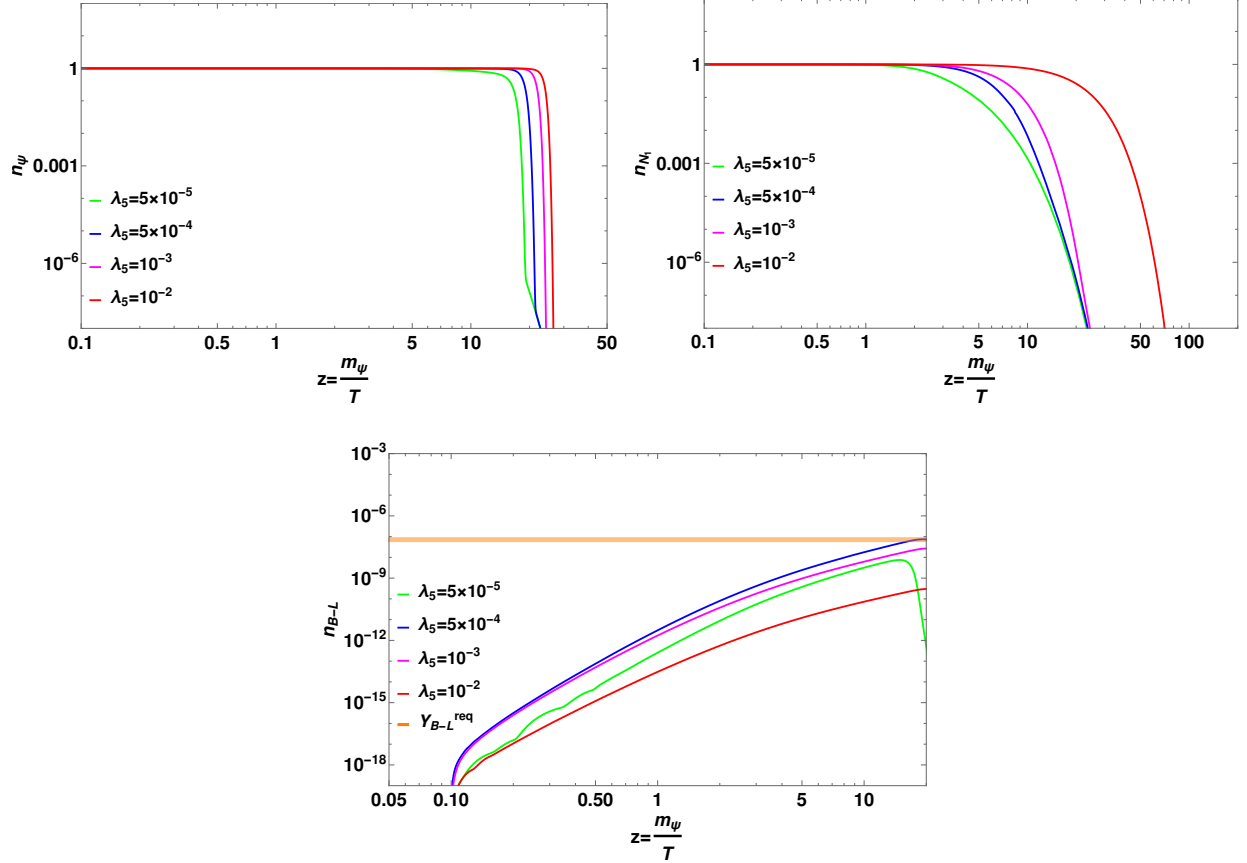


FIG. 5. Evolution of co-moving number density of  $\psi$  (upper left panel),  $N_1$  (upper right panel) and  $B - L$  (lower panel) with  $z = \frac{m_\psi}{T}$  for different values of  $\lambda_5$ . The other parameters are set at the following benchmark values  $M_1 = 4.101$  TeV,  $M_2 = 5$  TeV,  $m_{\eta_R} = 4.1$  TeV,  $m_S = 99.5$  GeV,  $m_\psi = 4.2$  TeV and  $y_1 = y_2^* = 10^{-4} + 10^{-4}i$ .

### 1. Case 1: $M_1 \approx m_\eta$

In this case we have first chosen a benchmark as  $M_1 = 4.101$  TeV,  $M_2 = 5$  TeV,  $m_\psi = 4.2$  TeV,  $m_S = 99.5$  GeV and  $m_{\eta_R} \approx 4.1$  TeV. We keep a small mass difference between  $M_1, m_{\eta_R}$  such that the decay width for the decay  $N_1 \rightarrow l\eta$  is very small and the lepton asymmetry is generated is mainly from the three body decay of  $\psi$ . Because of the smallness of  $M_1$  the washout process  $\psi\eta \rightarrow \ell S$  remains very strong thereby destroying the generated asymmetry significantly. For the sake of minimising this washout we have chosen the relevant Yukawa couplings of  $\psi - S - N_i$  vertices as  $y_1 = y_2^* = 10^{-4} + 10^{-4}i$ . As mentioned earlier, these couplings are free parameters and can be chosen independent of light neutrino masses.

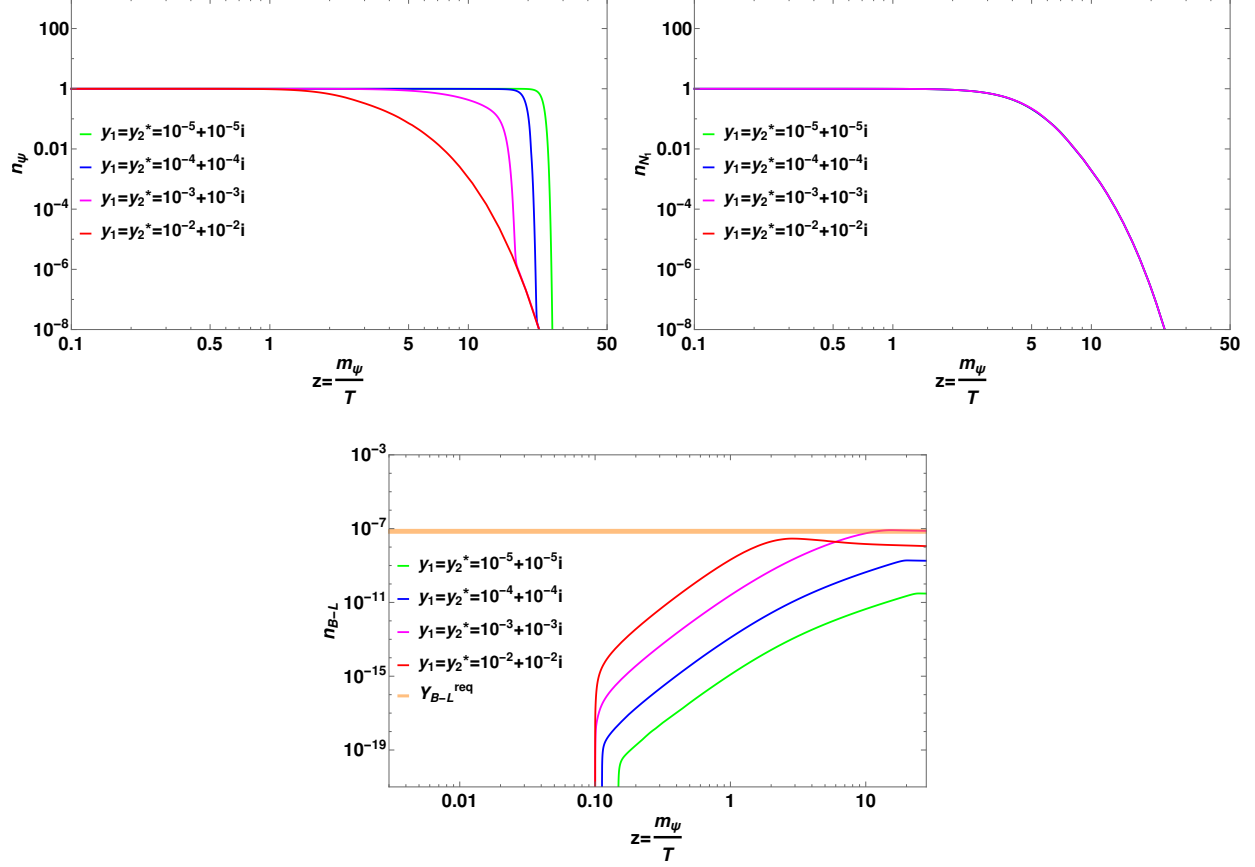


FIG. 6. Evolution of co-moving number density of  $\psi$  (upper left panel),  $N_1$  (upper right panel) and  $B - L$  (lower panel) with  $z = \frac{m_\psi}{T}$  for different values of  $y_{1,2}$ . The other parameters are set at the following benchmark values  $M_1 = 4.101$  TeV,  $M_2 = 5$  TeV,  $m_{\eta_R} = 4.1$  TeV,  $m_S = 99.5$  GeV,  $m_\psi = 4.2$  TeV and  $\lambda_5 = 10^{-3}$ .

Using this benchmark choice of relevant parameters, in figure 5, the evolution of the co-moving number densities of  $\psi$ ,  $N_1$  and  $B - L$  are shown with  $z = \frac{m_\psi}{T}$  for different values of  $\lambda_5$ . The parameter  $\lambda_5$  decided the strength of Dirac Yukawa coupling of neutrinos via Casas-Ibarra parametrisation (13) discussed earlier. In the bottom panel plot of figure 5, the lepton asymmetry increases initially with decrease in  $\lambda_5$ . With smaller values of  $\lambda_5$ , the Dirac Yukawa couplings are required to be larger in order to satisfy light neutrino masses (for fixed values of heavy neutrino masses  $M_i$ ) which increases the decay width  $\Gamma_{\psi \rightarrow lS\eta}$  responsible for creating the asymmetry. However, if we keep on decreasing  $\lambda_5$  further, at some point the Dirac Yukawa couplings become large enough to make the washout effects strong and thereby destroying the generated asymmetry.

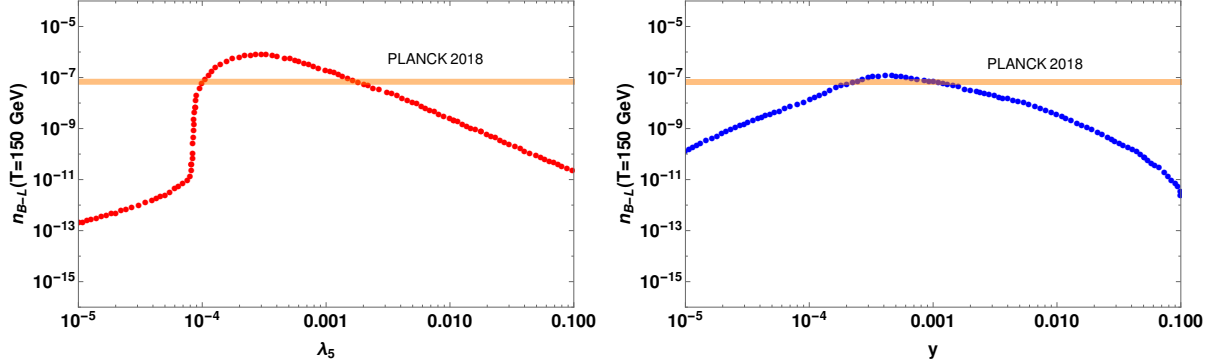


FIG. 7. Final B-L asymmetry with  $\lambda_5, y = |y_1| = |y_2^*|$  in case 1. The relevant parameters are fixed at the following benchmark values  $m_\psi = 4200$  GeV,  $m_{\eta_R} = 4100.5$  GeV,  $M_1 = 4100.7$  GeV,  $M_2 = 5000$  GeV and  $m_S = 99.4$  GeV. We fixed  $y_1 = y_2^* = 10^{-4} + 10^{-4}i$  (for the left panel plot) and  $\lambda_5 = 5 \times 10^{-4}$  (for the right panel plot).

In the decay width  $\Gamma_{\psi \rightarrow lS\eta}$ , apart from Dirac Yukawa couplings of neutrinos, we also have another Yukawa coupling  $y_{1,2}$  which can affect leptogenesis. In figure 6, we show the evolution of the co-moving number densities of  $\psi$ ,  $N_1$  and  $B - L$  with  $z = \frac{m_\psi}{T}$  are shown for different values of  $y_1$ . For simplicity, we keep  $y_2 = y_1^*$  although the results will not change significantly for a different choice. We choose the same benchmark as above for other relevant parameters while keeping  $\lambda_5$  fixed at  $10^{-3}$ . As we vary  $y_{1,2}$ , we see similar behaviour of asymmetry as it was noticed for different values of  $\lambda_5$  in figure 5. As can be seen from the bottom panel plot of figure 6, lepton asymmetry initially increases with increase in Yukawa couplings  $y_{1,2}$ . However, beyond a certain value of  $y_{1,2}$ , the washout processes become very strong to start depleting the asymmetry generated. Since  $y_{1,2}$  do not appear in the decay width of  $N_1$  into  $\eta, \ell$  and  $N_1$  decay into  $\psi, S$  is kinematically forbidden, the co-moving number density of  $N_1$  does not change if we choose different values of  $y_{1,2}$  as seen from upper right panel plot of figure 6.

After showing the evolution of co-moving number densities for different choices of parameters, we show the variation of final asymmetry around sphaleron decoupling temperature with the key parameters involved in two vertices of the three body decay  $\Gamma_{\psi \rightarrow lS\eta}$  namely,  $\lambda_5, y_{1,2}$  in figure 7. This clearly summarises the patterns observed in evolution of asymmetry shown for different benchmark values of  $\lambda_5, y_{1,2}$  in figure 5 and figure 6 discussed above. Increase (decrease) in  $y_{1,2}(\lambda_5)$  leads to increase in asymmetry till the washouts become

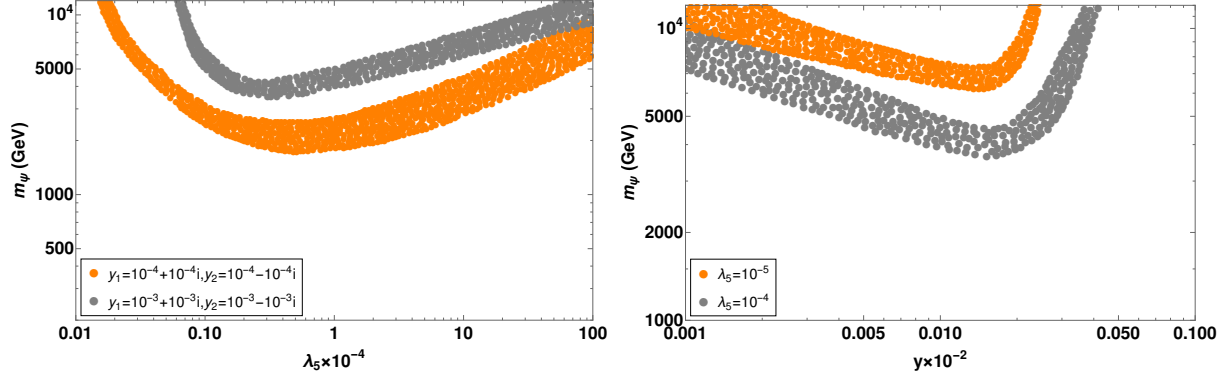


FIG. 8. Points satisfying the observed asymmetry in  $m_\psi$ - $\lambda_5$  plane (upper panel) and in  $m_\psi$ - $y$  plane (lower plane). The other parameters are fixed at  $m_S = 99.5$  GeV,  $m_{\eta_R} = m_\psi - m_S - 0.4$  GeV,  $M_1 = m_{\eta_R} + 0.5$  GeV.

dominant leading to depletion of asymmetry with further increase (decrease) of  $y_{1,2}(\lambda_5)$ . Finally, we perform a numerical scan to find the relevant parameter space  $m_\psi - \lambda_5 - y_{1,2}$  parameter space that can give rise to the observed baryon asymmetry. While varying these parameters, we keep the masses of other relevant particles to be fixed at  $m_S = 99.5$  GeV,  $m_{\eta_R} = m_\psi - m_S - 0.4$  GeV,  $M_1 = m_{\eta_R} + 0.5$  GeV. The parameter space in  $m_\psi - \lambda_5$  plane for benchmark choices of  $y_{1,2}$  is shown in left panel plot of figure 8. Clearly, for smaller benchmark choice of  $y_{1,2}$ , the scale of leptogenesis  $m_\psi$  can be below 2 TeV as well. The parameter space in  $m_\psi - y = |y_{1,2}|$  for benchmark choices of  $\lambda_5$  is shown on the right panel plot of figure 8 showing the possibility of low scale leptogenesis in the model.

### B. Case 2: $M_1 \gg m_\psi, m_\eta$

We now consider the case where  $N_{1,2}$  are much heavier than  $\psi, \eta$ . We choose  $M_1 = 5 \times 10^6$  GeV,  $M_2 = 10^7$  GeV and  $m_\eta = 1400$  GeV. The other parameters are fixed at benchmark values,  $m_\psi = 1500$  GeV,  $m_S = 50$  GeV. In this case the the lepton asymmetry generated by the  $N_1$  decay at high scale will be washed out by the washout processes operating at lower scale and finally the lepton asymmetry generated by the  $\psi$  decay will survive. The inverse decay  $l\eta \rightarrow N_1$  and the washout processes  $l\eta \rightarrow N_1, (W^\pm, Z)$  and  $ll \rightarrow N_1 N_1$  will be Boltzmann suppressed at the epoch of generation of lepton asymmetry from  $\psi$  decay. The washout processes  $\psi S \rightarrow l\eta$  and  $\psi\eta \rightarrow Sl$  are propagator suppressed compared to case 1.

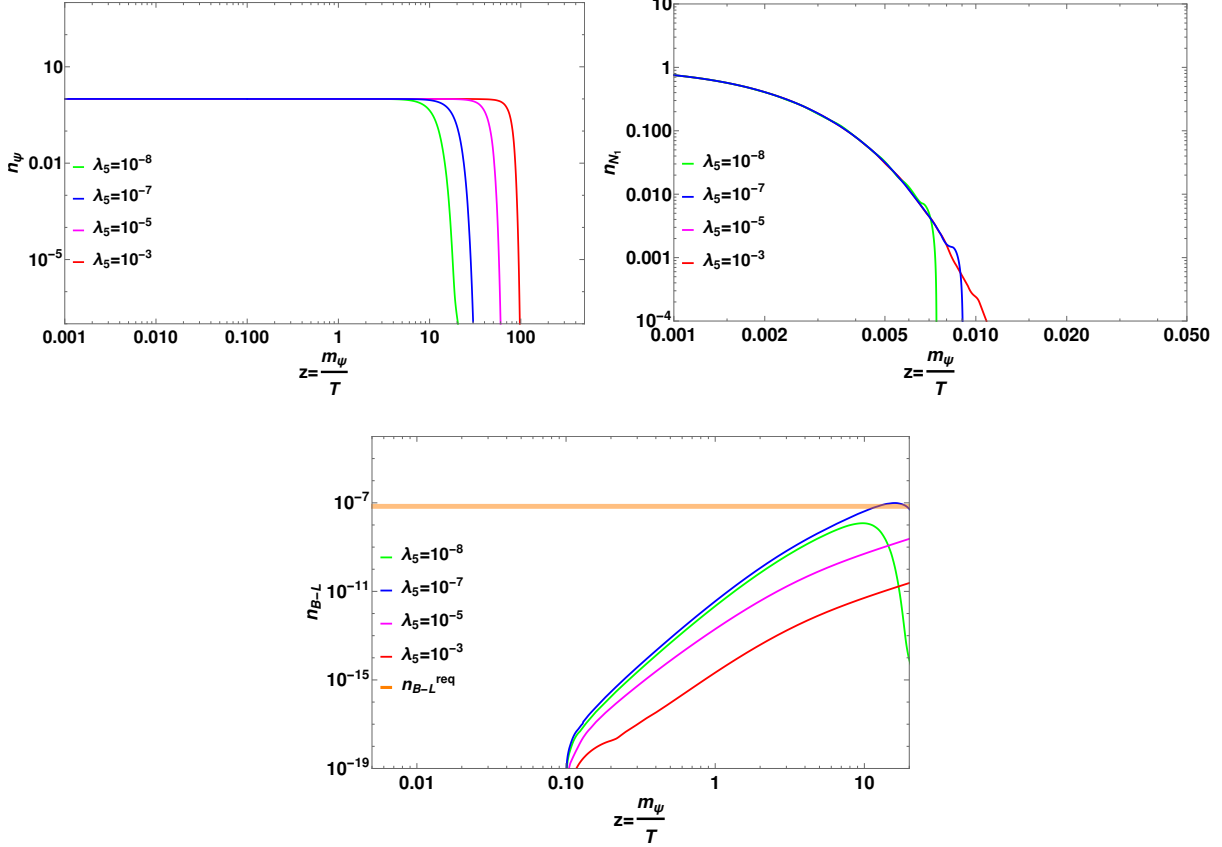


FIG. 9. Evolution of co-moving number density of  $\psi$  (upper left panel),  $N_1$  (upper right panel) and  $B - L$  (lower panel) with  $z = \frac{m_\psi}{T}$  for different values of  $\lambda_5$ . The other parameters are set at the following benchmark values  $M_1 = 5 \times 10^6$  GeV,  $M_2 = 10^7$  GeV,  $m_\eta = 1400$  GeV,  $m_S = 50$  GeV,  $m_\psi = 1500$  GeV and  $y_1 = 10^{-4} + 10^{-4}i$  and  $y_2 = 10^{-4} - 10^{-4}i$ .

The co-moving number densities of  $\psi$ ,  $N_1$  and  $B - L$  are shown with  $z = \frac{m_\psi}{T}$  for different values of  $\lambda_5$ ,  $y_{1,2}$  are shown in figure 9, 10 respectively. The variation of  $B - L$  asymmetry and the co-moving number density of  $\psi$  with  $\lambda_5$  as well as  $y_1$  are similar to the previous case discussed above. The behaviour of lepton asymmetry with different values of  $\lambda_5, y_{1,2}$  results due to the balance of creation of washout processes of lepton asymmetry, as noticed for case 1 as well. The number density of  $N_1$  is almost negligible near  $z \sim 1$ . Since  $N_1$  is very heavy, the Boltzmann suppression at lower temperatures is much more dominant than the change due to its decay width for different values of  $\lambda_5$ . Unlike in case 1, here we also notice some changes in  $N_1$  evolution for different values of  $y_{1,2}$  as seen from upper right panel of figure 10. This is because  $N_1$  decay into  $\psi, S$  is kinematically allowed for case 2. Therefore, larger

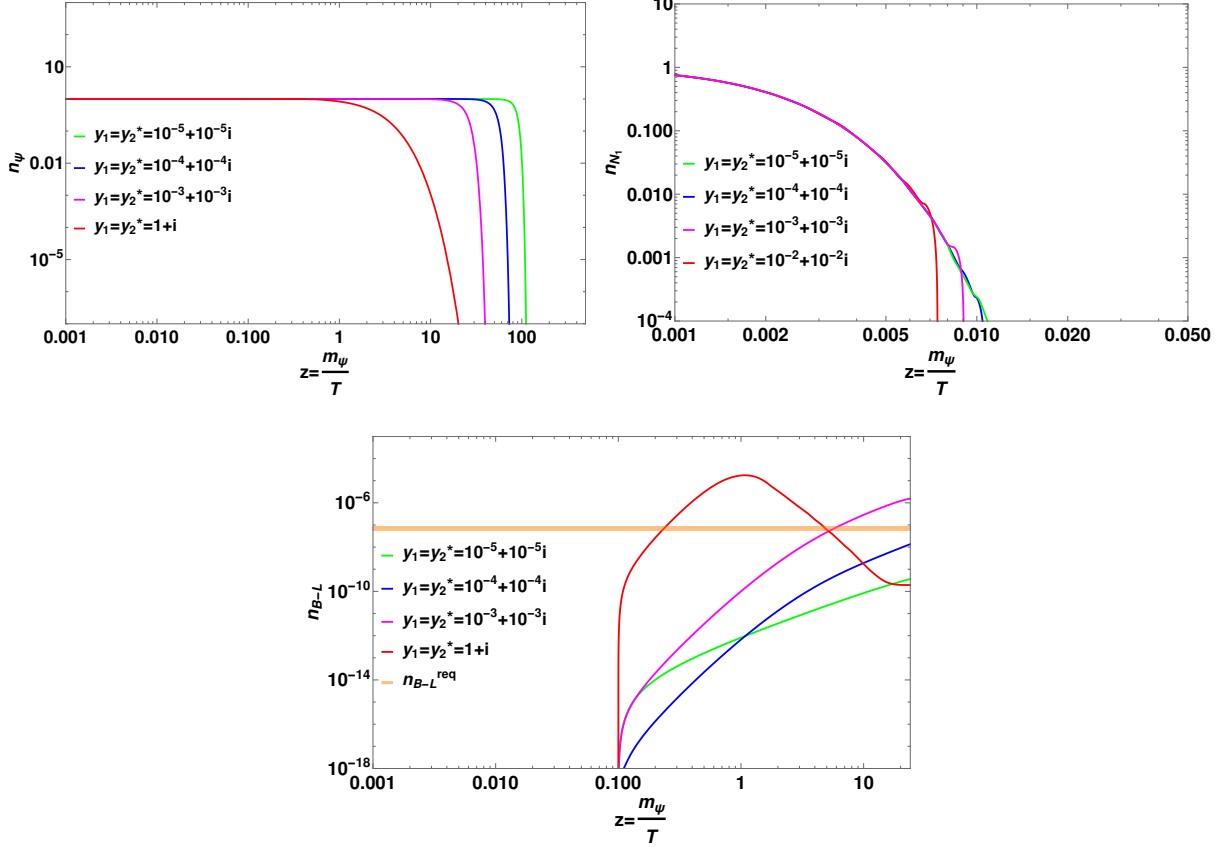


FIG. 10. Evolution of co-moving number density of  $\psi$  (upper left panel),  $N_1$  (upper right panel) and  $B - L$  (lower panel) with  $z = \frac{m_\psi}{T}$  for different values of  $y_1$ . The other parameters are set at the following benchmark values  $M_1 = 5 \times 10^6$  GeV,  $M_2 = 10^7$  GeV,  $m_\eta = 1400$  GeV,  $m_S = 50$  GeV,  $m_\psi = 1500$  GeV and  $\lambda_5 = 10^{-6}$ .

values of  $y_{1,2}$  lead to stronger depletion in  $N_1$  number density.

We then show the variation of final lepton asymmetry near sphaleron decoupling temperature with  $\lambda_5, y = |y_1| = |y_2^*|$  in figure 11. The behaviour remains similar to case 1 and can be explained with similar arguments. The final parameter space  $m_\psi - \lambda_5 - y_{1,2}$  that gives rise to successful leptogenesis is shown in figure 12. Clearly, the scale of leptogenesis can be as low as 1 TeV in this case. This is a significant improvement over the scale of leptogenesis obtained in minimal scotogenic model mentioned earlier.

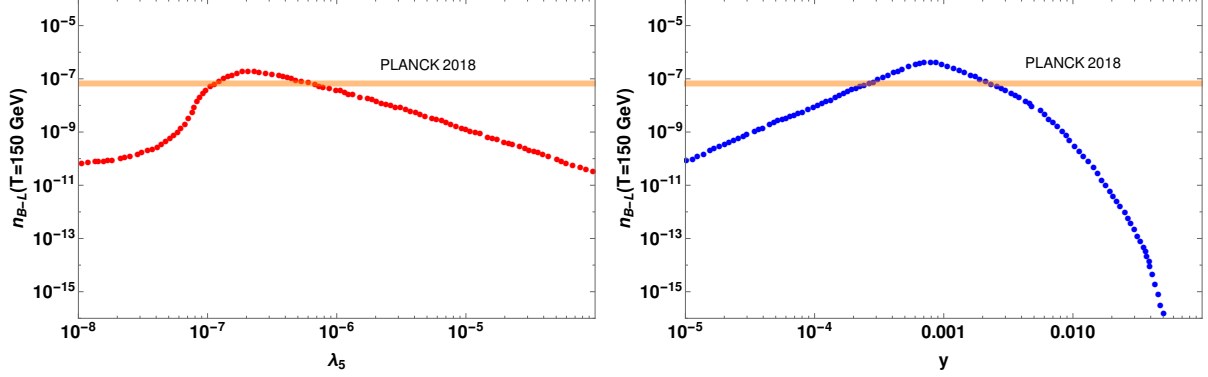


FIG. 11. Final B-L asymmetry with  $\lambda_5, y = |y_1| = |y_2^*|$  in case 2. The relevant parameters are fixed at the following benchmark values  $m_\psi = 4200$  GeV,  $m_{\eta_R} = 410$  GeV,  $M_1 = 5 \times 10^6$  GeV,  $M_2 = 10^7$  GeV and  $m_S = 99$  GeV. We have fixed  $y_1 = y_2^* = 10^{-4} + 10^{-4}i$  (for the left panel plot) and  $\lambda_5 = 3 \times 10^{-7}$  (for the right panel plot).

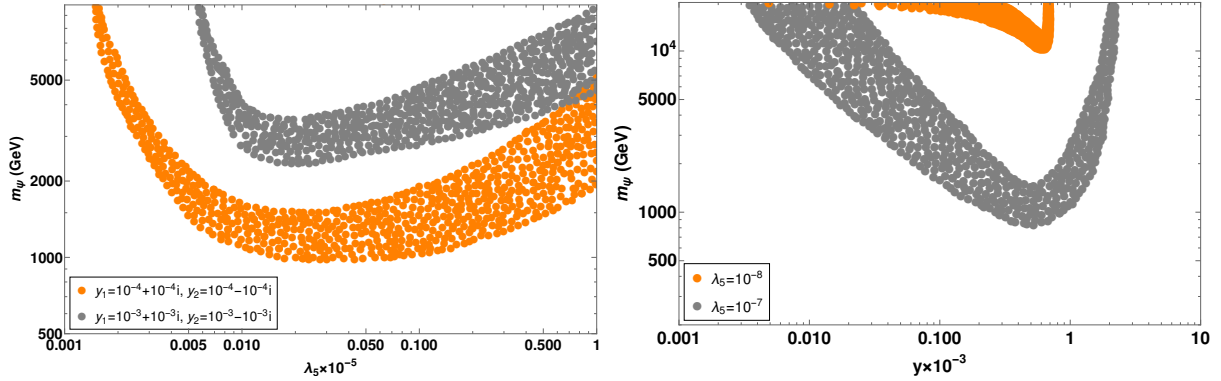


FIG. 12. Points satisfying the observed asymmetry in  $m_\psi$ - $\lambda_5$  plane (upper panel) and in  $m_\psi$ - $y$  plane (lower plane). The other parameters are set at the following benchmark values  $M_1 = 5 \times 10^6$  GeV,  $M_2 = 10^7$  GeV,  $m_\eta = 400$  GeV,  $m_S = 99$  GeV.

### C. Dark Matter

We briefly discuss our dark matter results in this subsection. As mentioned earlier, a two component scalar singlet and scalar doublet DM has been recently discussed in details within a type I seesaw model [72]. Instead of showing the details in general, here we focus on possible differences due to new couplings of these two DM candidates in relation to leptogenesis and neutrino mass as discussed above. We first discuss the behaviour of DM relic density with its mass for various possible combinations of relevant benchmark parameters. In figure 13,



we show the variation in individual and total DM relic densities for different mass relations between two DM candidates. While the overall features agree with the known results of scalar singlet and scalar doublet DM, there are some interesting differences due to inter-conversions and coannihilations here which we highlight.

In top left panel of figure 13, the two DM candidates are assumed to have equal masses. While the Higgs portal interactions of both the DM candidates are open due to the chosen non-zero couplings  $\lambda_6$ ,  $\lambda_L = \lambda_3 + \lambda_4 + \lambda_5$ . Although the Higgs portal coupling of doublet DM is relatively smaller, the coannihilation channels are very efficient due to tiny mass splittings  $\Delta m_{\eta_I} = m_{\eta_I} - m_{\eta_R}$ ,  $\Delta m_{\eta^\pm} = m_{\eta^\pm} - m_{\eta_R}$ , keeping its relic abundance suppressed compared to the singlet DM. In the top right panel plot of figure 13, a noticeable change in doublet DM relic abundance is observed. While all relevant couplings have the same value as those on the top left panel plot, the doublet DM relic increases as singlet DM mass is twice the mass of doublet DM and hence there can be efficient conversions from singlet to doublet DM through Higgs portal interactions. Note that in both of these plots, the direct conversion coupling  $\lambda_7$  is switched off and hence all possible DM conversions can occur only via Higgs portal interactions. To show the effect of DM conversion more clearly, we keep the mass of doublet DM fixed in the bottom left panel plot of figure 13. As the singlet DM mass approaches the doublet DM mass, there is a sharp fall in its relic while at the same time the doublet relic increases due to relative conversions. In this plot, such conversions can occur via both Higgs portal and direct coupling  $\lambda_7$ . Finally, on the bottom right panel of figure 13, we show one interesting feature where doublet DM relic density suddenly drops as its mass becomes close to 1.5 TeV. This particular feature is not due to DM conversions via Higgs portal or direct coupling  $\lambda_7$  as that can happen at any mass, given the fact that doublet mass is twice that of singlet mass all throughout. This happens due to doublet DM coannihilation with  $\psi$  whose mass is fixed at 1.5 TeV. Due to this coannihilation  $\eta_R \psi \rightarrow S \ell$ , the singlet relic density also increases, though it is not as prominent as the depletion of doublet relic density in the figure.

After discussing the general features of DM relic dependence on various relevant parameters, in figure 14, we specifically show the effects of direct conversion coupling  $\lambda_7$  and Yukawa coupling  $y_{1,2}$  of  $\psi - S - N_{1,2}$  vertices. Mass of doublet dark matter is assumed to be twice of singlet dark matter mass. Comparing top panel plots of figure 14 where  $y_{1,2} = 0$ , it is seen that turning on the direct conversion coupling  $\lambda_7$  leads to sharp fall in heavier DM relic

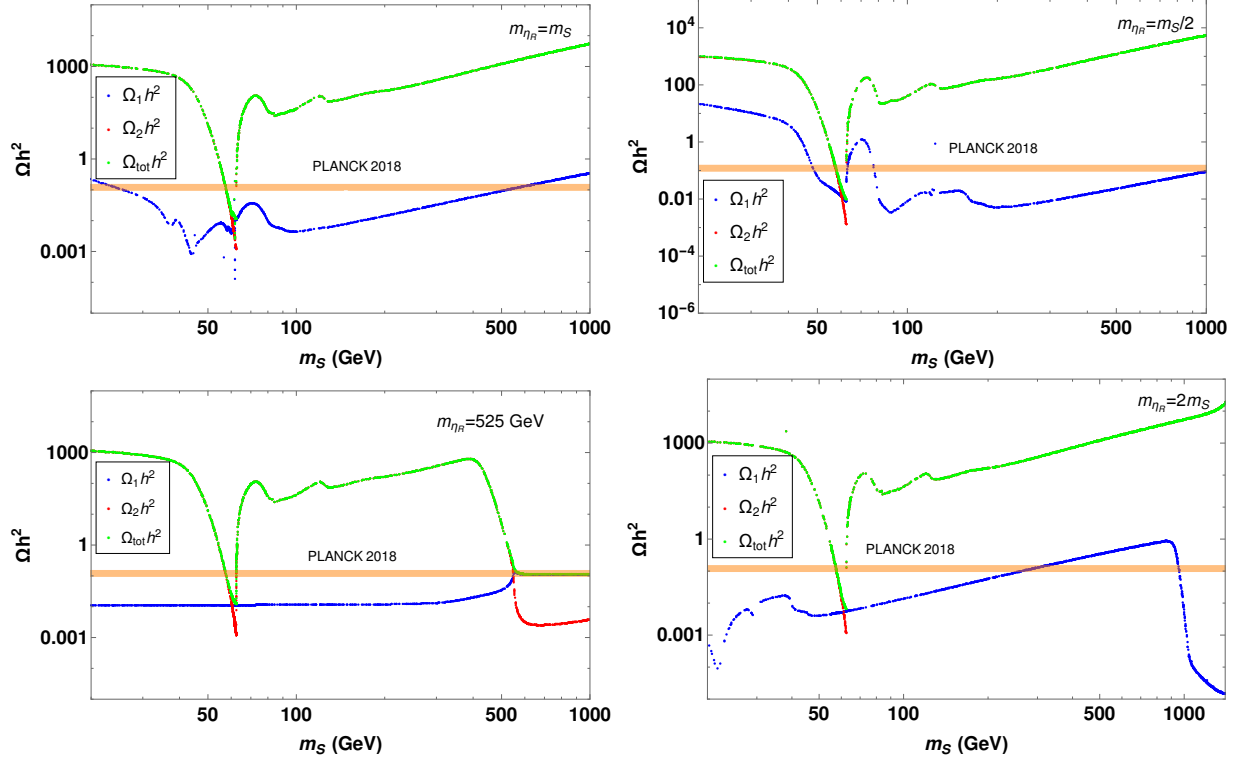


FIG. 13. Relic abundance versus DM mass for various mass relations between two DM candidates. The other parameters are fixed at the following benchmark values  $\lambda_L = 10^{-4}$ ,  $\lambda_6 = 10^{-3}$ ,  $\lambda_7 = 0$ ,  $y_{1,2} = 10^{-4}$ ,  $\Delta m_{\eta_I} = 2$  GeV and  $\Delta m_{\eta_{\pm}} = 2$  GeV.

density. Same effect is visible while comparing the bottom panel plots also where the effect of  $y_{1,2} \neq 0$  is also shown leading to depletion of doublet DM relic as its mass approaches  $m_{\psi}$ .

To find the relevant parameter space of DM that gives rise to the observed relic density, we perform a numerical scan for both the cases discussed in the context of leptogenesis namely case 1:  $M_1 \approx m_{\psi}, m_{\eta}$  and case 2:  $M_1 \gg m_{\psi}, m_{\eta}$ . For case 1, the parameter space in terms of two DM masses is shown on left panel plot of figure 15. To be in agreement with the parameter space chosen for leptogenesis, here we fix  $m_{\eta_R} < m_{\psi}$ ,  $m_S = m_{\psi} - m_{\eta_R} - 0.4$  GeV,  $M_1 = m_{\eta_R} + 0.5$  GeV,  $M_2 = M_1 + 1000$  GeV,  $m_{\eta_I} = m_{\eta_R} + 0.2$  GeV,  $m_{\eta_{\pm}} = m_{\eta_I} + 0.2$  GeV. The conversion coupling between the two DMs is varied between  $10^{-5} - 1$ . While singlet DM masses are evenly distributed across the range, there seems to be an upper bound on doublet DM mass near 400 GeV. This is due to the chosen mass splitting within doublet components. As earlier studies of inert scalar doublet DM shows [21, 58, 106–119],

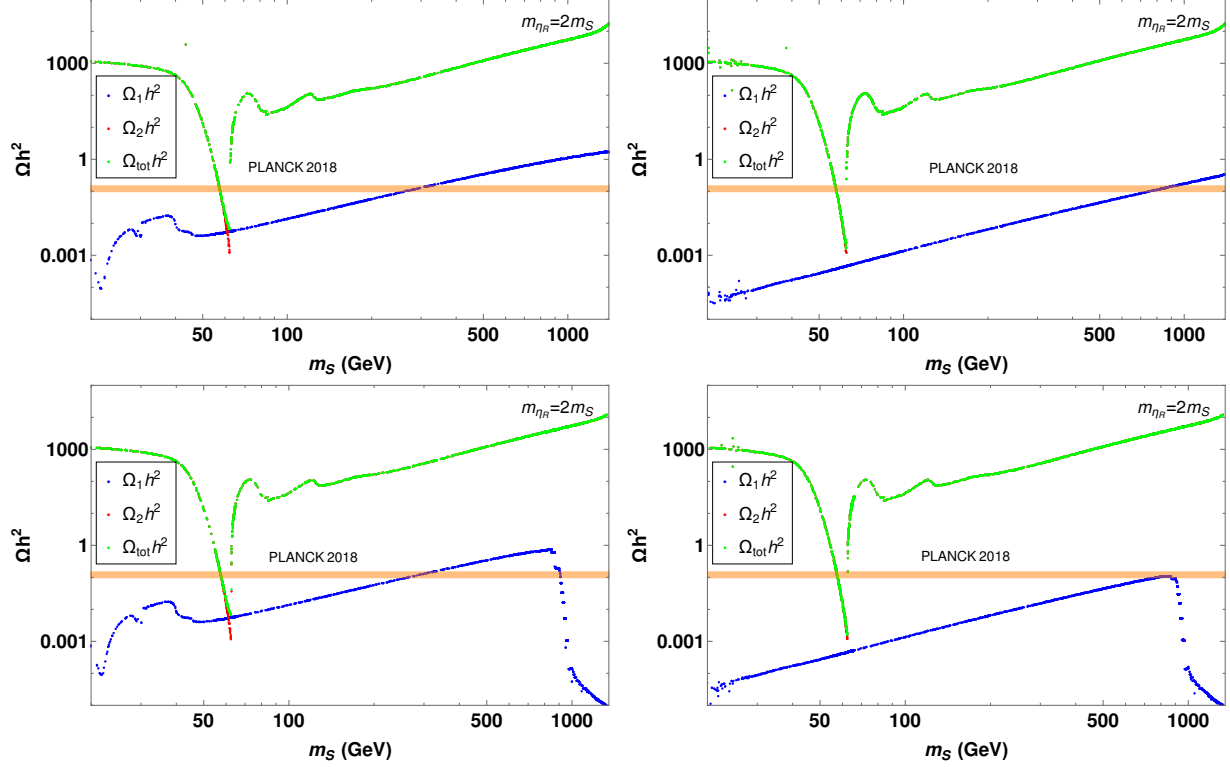


FIG. 14. Relic abundance versus DM mass showing the effects of direct conversion coupling  $\lambda_7$  and Yukawa coupling  $y_{1,2}$  of  $\psi - S - N_{1,2}$  vertices. The benchmark parameters fixed for all the four plots are  $\lambda_6 = 10^{-3}$  and  $\lambda_L = 10^{-4}$ . The conversion coupling and the new Yukawa coupling are fixed at  $y_{1,2} = 0$ ,  $\lambda_7 = 0$  (upper left panel plot),  $y_{1,2} = 0$ ,  $\lambda_7 = 1$  (upper right panel plot),  $y_{1,2} = 10^{-2}$ ,  $\lambda_7 = 0$  (lower left panel plot)  $y_{1,2} = 10^{-2}$ ,  $\lambda_7 = 1$  (lower right panel plot).

for such small mass splitting, the DM is overproduced in the high mass regime. While underproduction of one DM component in our model can be compensated by the second DM component, overabundance of one is difficult to reconcile with. Choosing a larger mass splitting within inert doublet components will allow more region of parameter space in terms of doublet DM mass. The right panel plot of figure 15 shows the spin independent DM-nucleon scattering rate of both the DM components, compared against the latest bound from Xenon1T experiment [130]. Clearly, all the points satisfy the direct detection bounds. This is due to the fact that, we have kept the Higgs portal coupling of both the DM candidates fixed at  $10^{-3}$ . Since tree level DM-nucleon scattering arises through Higgs portal couplings only, the corresponding rates remain low enough to survive Xenon1T bounds. The colour code on left panel plot of figure 15 shows the value of  $y = |y_1| = |y_2^*|$ . Similar scan plot for

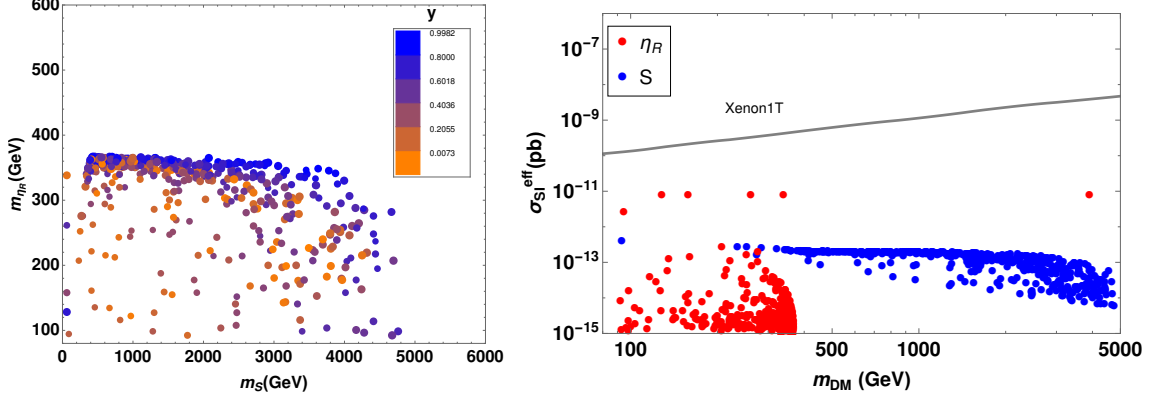


FIG. 15. Scan plot showing the parameter space in  $m_S - m_{\eta_R}$  plane allowed from total DM relic abundance (left panel) and  $m_{DM} - \sigma_{SI}$  plot for all the points satisfying the total relic (right panel). Following conditions are set for the scan  $m_{\eta_R} < m_\psi$ ,  $m_S = m_\psi - m_{\eta_R} - 0.4$  GeV,  $M_1 = m_{\eta_R} + 0.5$  GeV,  $M_2 = M_1 + 1000$  GeV,  $m_{\eta_I} = m_{\eta_R} + 0.2$  GeV,  $m_{\eta_\pm} = m_{\eta_I} + 0.2$  GeV. The conversion coupling between the two DMs is varied between  $10^{-5} - 1$ .

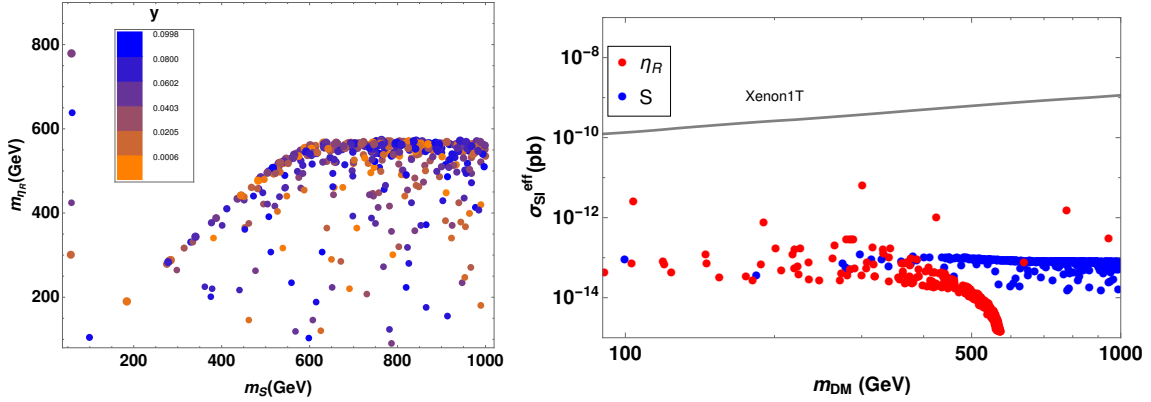


FIG. 16. Scan plot showing the parameter space in  $m_S - m_{\eta_R}$  plane allowed from total DM relic abundance (left panel) and  $m_{DM} - \sigma_{SI}$  plot for all the points satisfying the total relic (right panel). The other parameters are fixed at following benchmark values  $m_{\eta_I} = m_{\eta_R} + 2$  GeV,  $m_{\eta_\pm} = m_{\eta_I} + 2$  GeV,  $M_1 = 5 \times 10^6$  GeV and  $M_2 = 10^7$  GeV. The conversion coupling between the two DMs is varied between  $10^{-5} - 1$ .

case 2 is shown on the left panel of figure 16. The benchmark values of other parameters are  $m_{\eta_I} = m_{\eta_R} + 2$  GeV,  $m_{\eta_\pm} = m_{\eta_I} + 2$  GeV,  $M_1 = 5 \times 10^6$  GeV and  $M_2 = 10^7$  GeV,  $\lambda_7 \in (10^{-5} - 1)$ . While we notice a similar upper bound on doublet DM mass due to chosen mass splitting, the parameter space remains safe from direct detection bounds.

## VI. CONCLUSION

We have proposed a first of its kind model to implement the idea of leptogenesis from three body decay of a heavy particle where non-zero CP asymmetry arises due to interference of multiple tree level diagrams. Adopting a minimal framework to implement the idea, we augment the standard model of particle physics by three singlet fermions and two scalar fields: one singlet and one doublet. While two of these singlet fermions and the additional scalar doublet help in generating light neutrino masses one one loop level, the other two particles help in realising the desired three body decay leptogenesis. The two singlet fermions taking part in radiative neutrino mass generation also act like mediators in two different three body decay diagrams the interference of which results in the required non-zero CP asymmetry. It turns out that this setup automatically gives rise to a two component dark matter scenario in terms of scalar singlet and neutral component of scalar doublet. After deriving the particle spectrum of the model and applying the theoretical as well as experimental bounds, we calculate the CP asymmetry from three body decay of heavy singlet fermion by considering interference of two different diagrams. We then solve the Boltzmann equations relevant for leptogenesis incorporating the sources of lepton asymmetry as well as washouts to obtain the parameter space that can give rise to successful leptogenesis. After analysing the role or effects of some key parameters on generation of lepton asymmetry, we performed a numerical scan and show that successful leptogenesis can occur at a scale as low as 1 TeV. This is a factor of around 10 lower than the scale of leptogenesis in minimal scotogenic model considering two body decay of hierarchical heavy neutrinos studied in earlier works [21–30]. Such low scale leptogenesis possibility could have tantalising prospects of being probed at ongoing or near future experiments. After finding the parameter space that gives rise to successful TeV scale leptogenesis, we calculate the relic abundance of two DM components. Since such two component scalar DM have been already studied in earlier works, we focus primarily on the role of new parameters involving the two DM candidates in our model which also play non-trivial roles in leptogenesis. We first analyse these effects with benchmark choices of parameters and finally show the parameter space of two DM masses that is consistent with correct relic abundance and direct detection rates. Such a low scale model with two component DM, successful leptogenesis and light neutrino masses should face further scrutiny with future data from collider, neutrino, cosmology as well as

rare decay experiments looking for charged lepton flavour violation, neutrinoless double beta decay etc. While neutrinoless double beta decay contribution will effectively arise from light neutrino contributions only and will remain below the current experimental sensitivity of KamLAND-Zen experiment, i.e.,  $|m_{ee}| \leq (0.061 - 0.165)$  eV [136] for vanishing lightest neutrino mass. While charged lepton flavour violation like  $\mu \rightarrow e\gamma$ ,  $\mu \rightarrow 3e$  and  $\mu \rightarrow e$  (Ti) conversion in scotogenic models can be sizeable and saturate experimental upper bounds on corresponding branching ratios for fermion DM scenario [65, 137, 138], in our model they are likely to be suppressed as the singlet fermions  $N_{1,2}$  are heavier than the scale of leptogenesis. Another interesting prospect of probing our model can be in the form of gravitational waves from a strongly first order phase transition (SFOPT). In a recent work [138], it was shown that in the minimal scotogenic model, the criteria of SFOPT constrains the scalar sector a lot, leading to a scalar DM parameter space in tension with direct detection bounds. Due to the presence of an additional singlet scalar in our model whose mass is not as constrained as the inert doublet components, the SFOPT criteria is likely to be satisfied with more freedom. We leave a detailed study of this model from SFOPT point of view to future works.

## ACKNOWLEDGMENTS

DB acknowledges the support from Early Career Research Award from DST-SERB, Government of India (reference number: ECR/2017/001873).

## Appendix A: Three body decay of $\psi$

The amplitude squared of the decay process shown in figure 1 can be found to be

$$\begin{aligned}
\bar{\mathcal{M}}^2 = & \frac{|y_1|^2 |h_{1i}|^2}{(M_1^4 + M_1^2 \Gamma_1^2)} [2(p \cdot p_1)(p \cdot p_3) + 2m_\psi M_1(p \cdot p_3) + M_1^2(p_1 \cdot p_3) - p^2(p_1 \cdot p_3)] + \\
& \frac{|y_2|^2 |h_{2i}|^2}{(M_2^4 + M_2^2 \Gamma_2^2)} [2(p \cdot p_1)(p \cdot p_3) + 2m_\psi M_2(p \cdot p_3) + M_2^2(p_1 \cdot p_3) - p^2(p_1 \cdot p_3)] + \\
& \frac{\left(1 + \frac{\Gamma_1}{M_1} \frac{\Gamma_2}{M_2}\right) \text{Re}[y_1^* h_{i1}^* y_2 h_{i2}] + \left(\frac{\Gamma_1}{M_1} - \frac{\Gamma_2}{M_2}\right) \text{Im}[y_1^* h_{i1}^* y_2 h_{i2}]}{(M_1^2 + \Gamma_1^2)(M_2^2 + \Gamma_2^2)} \\
& [2(p \cdot p_1)(p \cdot p_3) + m_\psi(M_1 + M_2)(p \cdot p_3) + M_1 M_2(p_1 \cdot p_3) - p^2(p_1 \cdot p_3)],
\end{aligned} \tag{A1}$$

where  $p_1, p_2, p_3, p_4$  are the four momentum of  $\psi, S, \ell$  and  $\eta$  respectively.  $p = p_1 - p_2$  is the four momentum of the propagator.

The decay width of the process  $\psi \rightarrow Sl\eta$  under the approximation of massless final states is given by

$$\begin{aligned}
\Gamma_{\psi \rightarrow Sl\eta} &= \frac{|y_1|^2 |h_{1i}|^2}{128\pi^3} \frac{1}{\left(1 + \frac{\Gamma_1^2}{M_1^2}\right)} \left(\frac{m_\psi^5}{48M_1^4}\right) \left[1 + \frac{4M_1^2}{m_\psi^2}\right] + \frac{|y_2|^2 |h_{2i}|^2}{128\pi^3} \frac{1}{\left(1 + \frac{\Gamma_2^2}{M_2^2}\right)} \left(\frac{m_\psi^5}{48M_2^4}\right) \\
&\times \left[1 + \frac{4M_2^2}{m_\psi^2}\right] + \frac{\left(1 + \frac{\Gamma_1}{M_1} \frac{\Gamma_2}{M_2}\right) \text{Re}(y_1^* h_{i1}^* y_2 h_{i2}) + \left(\frac{\Gamma_1}{M_1} - \frac{\Gamma_2}{M_2}\right) \text{Im}(y_1^* h_{i1}^* y_2 h_{i2}^*)}{128\pi^3} \\
&\times \frac{1}{\left(1 + \frac{\Gamma_1^2}{M_1^2}\right) \left(1 + \frac{\Gamma_2^2}{M_2^2}\right)} \left(\frac{m_\psi^5}{48M_1^2 M_2^2}\right) \left[1 + \frac{4M_1 M_2}{m_\psi^2}\right]. \tag{A2}
\end{aligned}$$

The CP asymmetry parameter associated with the decay  $\psi \rightarrow Sl\eta$  is found out to be

$$\begin{aligned}
\epsilon_\psi &= \left[ \frac{\left(\frac{\Gamma_1}{M_1} - \frac{\Gamma_2}{M_2}\right) \left(\frac{m_\psi^5}{24M_1^2 M_2^2}\right) \left[1 + \frac{4M_1 M_2}{m_\psi^2}\right]}{\left(1 + \frac{\Gamma_1^2}{M_1^2}\right) \left(1 + \frac{\Gamma_2^2}{M_2^2}\right)} \text{Im}[y_1^* h_{i1}^* y_2 h_{i2}] \right] \\
&\times \left[ \frac{|y_1|^2 |h_{1i}|^2}{\left(1 + \frac{\Gamma_1^2}{M_1^2}\right)} \left(\frac{m_\psi^5}{24M_1^4}\right) \left[1 + \frac{4M_1^2}{m_\psi^2}\right] + \frac{|y_2|^2 |h_{2i}|^2}{\left(1 + \frac{\Gamma_2^2}{M_2^2}\right)} \left(\frac{m_\psi^5}{24M_2^4}\right) \left[1 + \frac{4M_2^2}{m_\psi^2}\right] \right. \\
&\left. + \frac{\left(1 + \frac{\Gamma_1}{M_1} \frac{\Gamma_2}{M_2}\right) \left(\frac{m_\psi^5}{24M_1^2 M_2^2}\right) \left[1 + \frac{4M_1 M_2}{m_\psi^2}\right]}{\left(1 + \frac{\Gamma_1^2}{M_1^2}\right) \left(1 + \frac{\Gamma_2^2}{M_2^2}\right)} \text{Re}[y_1^* h_{i1}^* y_2 h_{i2}] \right]^{-1}. \tag{A3}
\end{aligned}$$

While SM lepton mass can be neglected, the masses of  $S, \eta$  can be comparable to that of  $\psi$ . If we consider one their masses (say,  $m_S$ ) to be comparable to that of  $\psi$  and denote the mass difference as  $\Delta_\psi = m_\psi - m_S$ , in the above expressions  $m_\psi^5$  will be replaced by  $\Delta_\psi^5$ .

## Appendix B: Two body decay of $N_i$

The decay width for the decay  $N_1 \rightarrow \eta l$  is given by

$$\Gamma_{N_1 \rightarrow \eta l} = \frac{M_1}{8\pi} (h^\dagger h)_{11} \left(1 - \frac{m_\eta^2}{M_1^2}\right)^2 \tag{B1}$$

The CP asymmetry parameter for  $N_i \rightarrow l_\alpha \eta, \bar{l}_\alpha \bar{\eta}$  is given by

$$\epsilon_{i\alpha} = \frac{1}{8\pi(h^\dagger h)_{ii}} \sum_{j \neq i} \left[ f\left(\frac{M_j^2}{M_i^2}, \frac{m_\eta^2}{M_i^2}\right) \text{Im}[h_{\alpha i}^* h_{\alpha j} (h^\dagger h)_{ij}] - \frac{M_i^2}{M_j^2 - M_i^2} \left(1 - \frac{m_\eta^2}{M_i^2}\right)^2 \text{Im}[h_{\alpha i}^* h_{\alpha j} H_{ij}] \right] \quad (\text{B2})$$

where, the function  $f(r_{ji}, \eta_i)$  is coming from the interference of the tree-level and one loop diagrams and has the form

$$f(r_{ji}, \eta_i) = \sqrt{r_{ji}} \left[ 1 + \frac{(1 - 2\eta_i + r_{ji})}{(1 - \eta_i^2)^2} \ln\left(\frac{r_{ji} - \eta_i^2}{1 - 2\eta_i + r_{ji}}\right) \right] \quad (\text{B3})$$

with  $r_{ji} = M_j^2/M_i^2$  and  $\eta_i = m_\eta^2/M_i^2$ . The self energy contribution  $H_{ij}$  is given by

$$H_{ij} = (h^\dagger h)_{ij} \frac{M_j}{M_i} + (h^\dagger h)_{ij}^* \quad (\text{B4})$$

Now, the CP asymmetry parameter, neglecting the flavour effects (summing over final state flavours  $\alpha$ ) is

$$\epsilon_i = \frac{1}{8\pi(h^\dagger h)_{ii}} \sum_{j \neq i} \text{Im}[(h^\dagger h)_{ij}]^2 \frac{1}{\sqrt{r_{ji}}} F(r_{ji}, \eta_i) \quad (\text{B5})$$

where the function  $F(r_{ji}, \eta)$  is defined as

$$F(r_{ji}, \eta_i) = \sqrt{r_{ji}} \left[ f(r_{ji}, \eta_i) - \frac{\sqrt{r_{ji}}}{r_{ji} - 1} (1 - \eta_i)^2 \right]. \quad (\text{B6})$$

- [1] **Particle Data Group** Collaboration, M. Tanabashi et al., *Review of Particle Physics*, *Phys. Rev. D* **98** (2018), no. 3 030001.
- [2] **Planck** Collaboration, N. Aghanim et al., *Planck 2018 results. VI. Cosmological parameters*, [arXiv:1807.06209](https://arxiv.org/abs/1807.06209).
- [3] A. D. Sakharov, *Violation of CP Invariance, C asymmetry, and baryon asymmetry of the universe*, *Pisma Zh. Eksp. Teor. Fiz.* **5** (1967) 32–35. [*Usp. Fiz. Nauk*161,no.5,61(1991)].
- [4] S. Weinberg, *Cosmological Production of Baryons*, *Phys. Rev. Lett.* **42** (1979) 850–853.
- [5] E. W. Kolb and S. Wolfram, *Baryon Number Generation in the Early Universe*, *Nucl. Phys.* **B172** (1980) 224. [Erratum: *Nucl. Phys.*B195,542(1982)].
- [6] V. A. Kuzmin, V. A. Rubakov, and M. E. Shaposhnikov, *On the Anomalous Electroweak Baryon Number Nonconservation in the Early Universe*, *Phys. Lett.* **155B** (1985) 36.



- [7] M. Fukugita and T. Yanagida, *Baryogenesis Without Grand Unification*, *Phys. Lett.* **B174** (1986) 45–47.
- [8] S. Davidson, E. Nardi, and Y. Nir, *Leptogenesis*, *Phys. Rept.* **466** (2008) 105–177, [[arXiv:0802.2962](#)].
- [9] P. Minkowski,  $\mu \rightarrow e\gamma$  at a Rate of One Out of  $10^9$  Muon Decays?, *Phys. Lett.* **B67** (1977) 421–428.
- [10] R. N. Mohapatra and G. Senjanovic, *Neutrino Mass and Spontaneous Parity Violation*, *Phys. Rev. Lett.* **44** (1980) 912.
- [11] T. Yanagida, *HORIZONTAL SYMMETRY AND MASSES OF NEUTRINOS*, *Conf. Proc.* **C7902131** (1979) 95–99.
- [12] M. Gell-Mann, P. Ramond, and R. Slansky, *Complex Spinors and Unified Theories*, *Conf. Proc.* **C790927** (1979) 315–321, [[arXiv:1306.4669](#)].
- [13] S. L. Glashow, *The Future of Elementary Particle Physics*, *NATO Sci. Ser. B* **61** (1980) 687.
- [14] J. Schechter and J. W. F. Valle, *Neutrino Masses in  $SU(2) \times U(1)$  Theories*, *Phys. Rev.* **D22** (1980) 2227.
- [15] F. Zwicky, *Die Rotverschiebung von extragalaktischen Nebeln*, *Helv. Phys. Acta* **6** (1933) 110–127. [Gen. Rel. Grav.41,207(2009)].
- [16] V. C. Rubin and W. K. Ford, Jr., *Rotation of the Andromeda Nebula from a Spectroscopic Survey of Emission Regions*, *Astrophys. J.* **159** (1970) 379–403.
- [17] D. Clowe, M. Bradac, A. H. Gonzalez, M. Markevitch, S. W. Randall, C. Jones, and D. Zaritsky, *A direct empirical proof of the existence of dark matter*, *Astrophys. J.* **648** (2006) L109–L113, [[astro-ph/0608407](#)].
- [18] E. W. Kolb and M. S. Turner, *The Early Universe*, *Front. Phys.* **69** (1990) 1–547.
- [19] G. Arcadi, M. Dutra, P. Ghosh, M. Lindner, Y. Mambrini, M. Pierre, S. Profumo, and F. S. Queiroz, *The Waning of the WIMP? A Review of Models, Searches, and Constraints*, [[arXiv:1703.07364](#)].
- [20] E. Ma, *Verifiable radiative seesaw mechanism of neutrino mass and dark matter*, *Phys. Rev.* **D73** (2006) 077301, [[hep-ph/0601225](#)].
- [21] T. Hambye, F. S. Ling, L. Lopez Honorez, and J. Rocher, *Scalar Multiplet Dark Matter*, *JHEP* **07** (2009) 090, [[arXiv:0903.4010](#)]. [Erratum: JHEP05,066(2010)].

- [22] J. Racker, *Mass bounds for baryogenesis from particle decays and the inert doublet model*, *JCAP* **1403** (2014) 025, [[arXiv:1308.1840](#)].
- [23] J. D. Clarke, R. Foot, and R. R. Volkas, *Natural leptogenesis and neutrino masses with two Higgs doublets*, *Phys. Rev.* **D92** (2015), no. 3 033006, [[arXiv:1505.05744](#)].
- [24] T. Hugle, M. Platscher, and K. Schmitz, *Low-Scale Leptogenesis in the Scotogenic Neutrino Mass Model*, *Phys. Rev.* **D98** (2018), no. 2 023020, [[arXiv:1804.09660](#)].
- [25] D. Borah, P. S. B. Dev, and A. Kumar, *TeV scale leptogenesis, inflaton dark matter and neutrino mass in a scotogenic model*, *Phys. Rev.* **D99** (2019), no. 5 055012, [[arXiv:1810.03645](#)].
- [26] D. Mahanta and D. Borah, *Fermion dark matter with  $N_2$  leptogenesis in minimal scotogenic model*, *JCAP* **11** (2019) 021, [[arXiv:1906.03577](#)].
- [27] D. Mahanta and D. Borah, *TeV Scale Leptogenesis with Dark Matter in Non-standard Cosmology*, *JCAP* **04** (2020), no. 04 032, [[arXiv:1912.09726](#)].
- [28] L. Sarma, P. Das, and M. K. Das, *Scalar dark matter, leptogenesis and  $0\nu\beta\beta$  in minimal scotogenic model*, [[arXiv:2004.13762](#)].
- [29] S. Kashiwase and D. Suematsu, *Baryon number asymmetry and dark matter in the neutrino mass model with an inert doublet*, *Phys. Rev.* **D86** (2012) 053001, [[arXiv:1207.2594](#)].
- [30] S. Kashiwase and D. Suematsu, *Leptogenesis and dark matter detection in a TeV scale neutrino mass model with inverted mass hierarchy*, *Eur. Phys. J.* **C73** (2013) 2484, [[arXiv:1301.2087](#)].
- [31] S. Davidson and A. Ibarra, *A Lower bound on the right-handed neutrino mass from leptogenesis*, *Phys. Lett.* **B535** (2002) 25–32, [[hep-ph/0202239](#)].
- [32] A. Masiero and A. Riotto, *Cosmic Delta B from lepton violating interactions at the electroweak phase transition*, *Phys. Lett. B* **289** (1992) 73–80, [[hep-ph/9206212](#)].
- [33] R. Adhikari and U. Sarkar, *Baryogenesis in a supersymmetric model without R-parity*, *Phys. Lett. B* **427** (1998) 59–64, [[hep-ph/9610221](#)].
- [34] U. Sarkar and R. Adhikari, *Baryogenesis through R-parity violation*, *Phys. Rev. D* **55** (1997) 3836–3843, [[hep-ph/9608209](#)].
- [35] T. Hambye, *Leptogenesis at the TeV scale*, *Nucl. Phys. B* **633** (2002) 171–192, [[hep-ph/0111089](#)].
- [36] A. Dasgupta, P. Bhupal Dev, S. K. Kang, and Y. Zhang, *Matter-antimatter asymmetry*

- without loops, [arXiv:1911.03013](#).
- [37] W. Abdallah, A. Kumar, and A. K. Saha, *Soft leptogenesis in the NMSSM with a singlet right-handed neutrino superfield*, *JHEP* **04** (2020) 065, [[arXiv:1911.03363](#)].
- [38] Y. Grossman, T. Kashti, Y. Nir, and E. Roulet, *Leptogenesis from supersymmetry breaking*, *Phys. Rev. Lett.* **91** (2003) 251801, [[hep-ph/0307081](#)].
- [39] G. D'Ambrosio, G. F. Giudice, and M. Raidal, *Soft leptogenesis*, *Phys. Lett. B* **575** (2003) 75–84, [[hep-ph/0308031](#)].
- [40] C. S. Fong, M. Gonzalez-Garcia, and E. Nardi, *Leptogenesis from Soft Supersymmetry Breaking (Soft Leptogenesis)*, *Int. J. Mod. Phys. A* **26** (2011) 3491–3604, [[arXiv:1107.5312](#)].
- [41] D. Borah and R. Adhikari, *Abelian Gauge Extension of Standard Model: Dark Matter and Radiative Neutrino Mass*, *Phys. Rev. D* **85** (2012) 095002, [[arXiv:1202.2718](#)].
- [42] R. Adhikari, D. Borah, and E. Ma, *New  $U(1)$  Gauge Model of Radiative Lepton Masses with Sterile Neutrino and Dark Matter*, *Phys. Lett. B* **755** (2016) 414–417, [[arXiv:1512.05491](#)].
- [43] D. Nanda and D. Borah, *Common origin of neutrino mass and dark matter from anomaly cancellation requirements of a  $U(1)_{B-L}$  model*, *Phys. Rev.* **D96** (2017), no. 11 115014, [[arXiv:1709.08417](#)].
- [44] B. Barman, D. Borah, P. Ghosh, and A. K. Saha, *Flavoured gauge extension of singlet-doublet fermionic dark matter: neutrino mass, high scale validity and collider signatures*, *JHEP* **10** (2019) 275, [[arXiv:1907.10071](#)].
- [45] A. Biswas, D. Borah, and D. Nanda, *Type III seesaw for neutrino masses in  $U(1)_{B-L}$  model with multi-component dark matter*, *JHEP* **12** (2019) 109, [[arXiv:1908.04308](#)].
- [46] D. Nanda and D. Borah, *Connecting Light Dirac Neutrinos to a Multi-component Dark Matter Scenario in Gauged  $B - L$  Model*, *Eur. Phys. J. C* **80** (2020), no. 6 557, [[arXiv:1911.04703](#)].
- [47] A. Merle and M. Platscher, *Running of radiative neutrino masses: the scotogenic model revisited*, *JHEP* **11** (2015) 148, [[arXiv:1507.06314](#)].
- [48] P. F. de Salas, D. V. Forero, C. A. Ternes, M. Tortola, and J. W. F. Valle, *Status of neutrino oscillations 2018:  $3\sigma$  hint for normal mass ordering and improved CP sensitivity*, *Phys. Lett.* **B782** (2018) 633–640, [[arXiv:1708.01186](#)].
- [49] I. Esteban, M. C. Gonzalez-Garcia, A. Hernandez-Cabezudo, M. Maltoni, and T. Schwetz,

- Global analysis of three-flavour neutrino oscillations: synergies and tensions in the determination of  $\theta_{23}$ ,  $\delta_{CP}$ , and the mass ordering*, *JHEP* **01** (2019) 106, [[arXiv:1811.05487](#)].
- [50] J. A. Casas and A. Ibarra, *Oscillating neutrinos and muon  $\rightarrow e$ , gamma*, *Nucl. Phys.* **B618** (2001) 171–204, [[hep-ph/0103065](#)].
- [51] T. Toma and A. Vicente, *Lepton Flavor Violation in the Scotogenic Model*, *JHEP* **01** (2014) 160, [[arXiv:1312.2840](#)].
- [52] A. Ibarra and G. G. Ross, *Neutrino phenomenology: The Case of two right-handed neutrinos*, *Phys. Lett.* **B591** (2004) 285–296, [[hep-ph/0312138](#)].
- [53] E. Lundstrom, M. Gustafsson, and J. Edsjo, *The Inert Doublet Model and LEP II Limits*, *Phys. Rev.* **D79** (2009) 035013, [[arXiv:0810.3924](#)].
- [54] **ATLAS** Collaboration, M. Aaboud et al., *Combination of searches for invisible Higgs boson decays with the ATLAS experiment*, *Phys. Rev. Lett.* **122** (2019), no. 23 231801, [[arXiv:1904.05105](#)].
- [55] **ATLAS** Collaboration, *Search for invisible Higgs boson decays with vector boson fusion signatures with the ATLAS detector using an integrated luminosity of 139 fb<sup>-1</sup>*, .
- [56] D. Borah and A. Dasgupta, *Left Right Symmetric Models with a Mixture of keV-TeV Dark Matter*, [arXiv:1710.06170](#).
- [57] X. Miao, S. Su, and B. Thomas, *Trilepton Signals in the Inert Doublet Model*, *Phys. Rev. D* **82** (2010) 035009, [[arXiv:1005.0090](#)].
- [58] M. Gustafsson, S. Rydbeck, L. Lopez-Honorez, and E. Lundstrom, *Status of the Inert Doublet Model and the Role of multileptons at the LHC*, *Phys. Rev.* **D86** (2012) 075019, [[arXiv:1206.6316](#)].
- [59] A. Datta, N. Ganguly, N. Khan, and S. Rakshit, *Exploring collider signatures of the inert Higgs doublet model*, *Phys. Rev.* **D95** (2017), no. 1 015017, [[arXiv:1610.00648](#)].
- [60] P. Poullose, S. Sahoo, and K. Sridhar, *Exploring the Inert Doublet Model through the dijet plus missing transverse energy channel at the LHC*, *Phys. Lett.* **B765** (2017) 300–306, [[arXiv:1604.03045](#)].
- [61] M. Hashemi and S. Najjari, *Observability of Inert Scalars at the LHC*, [arXiv:1611.07827](#).
- [62] A. Belyaev, G. Cacciapaglia, I. P. Ivanov, F. Rojas, and M. Thomas, *Anatomy of the Inert Two Higgs Doublet Model in the light of the LHC and non-LHC Dark Matter Searches*,

[arXiv:1612.00511](#).

- [63] A. Belyaev, T. Fernandez Perez Tomei, P. Mercadante, C. Moon, S. Moretti, S. Novaes, L. Panizzi, F. Rojas, and M. Thomas, *Advancing LHC probes of dark matter from the inert two-Higgs-doublet model with the monojet signal*, *Phys. Rev. D* **99** (2019), no. 1 015011, [[arXiv:1809.00933](#)].
- [64] D. Borah, S. Sadhukhan, and S. Sahoo, *Lepton Portal Limit of Inert Higgs Doublet Dark Matter with Radiative Neutrino Mass*, [arXiv:1703.08674](#).
- [65] D. Borah, D. Nanda, N. Narendra, and N. Sahu, *Right-handed Neutrino Dark Matter with Radiative Neutrino Mass in Gauged  $B - L$  Model*, [arXiv:1810.12920](#).
- [66] M. Sher, *Electroweak Higgs Potentials and Vacuum Stability*, *Phys. Rept.* **179** (1989) 273–418.
- [67] K. Kannike, *Vacuum Stability Conditions From Copositivity Criteria*, *Eur. Phys. J. C* **72** (2012) 2093, [[arXiv:1205.3781](#)].
- [68] J. Chakraborty, P. Konar, and T. Mondal, *Copositive Criteria and Boundedness of the Scalar Potential*, *Phys. Rev. D* **89** (2014), no. 9 095008, [[arXiv:1311.5666](#)].
- [69] D. Borah, A. Dasgupta, and S. K. Kang, *Leptogenesis from Dark Matter Annihilations in Scotogenic Model*, [arXiv:1806.04689](#).
- [70] D. Borah, A. Dasgupta, and S. K. Kang, *Two-component dark matter withogenesis of the baryon asymmetry of the Universe*, *Phys. Rev. D* **100** (2019), no. 10 103502, [[arXiv:1903.10516](#)].
- [71] W.-C. Huang, H. Pas, and S. Zeissner, *Scalar Dark Matter, GUT baryogenesis and Radiative neutrino mass*, *Phys. Rev.* **D98** (2018), no. 7 075024, [[arXiv:1806.08204](#)].
- [72] S. Bhattacharya, P. Ghosh, A. K. Saha, and A. Sil, *Two component dark matter with inert Higgs doublet: neutrino mass, high scale validity and collider searches*, *JHEP* **03** (2020) 090, [[arXiv:1905.12583](#)].
- [73] Q.-H. Cao, E. Ma, J. Wudka, and C. P. Yuan, *Multipartite dark matter*, [arXiv:0711.3881](#).
- [74] K. M. Zurek, *Multi-Component Dark Matter*, *Phys. Rev.* **D79** (2009) 115002, [[arXiv:0811.4429](#)].
- [75] D. Chialva, P. S. B. Dev, and A. Mazumdar, *Multiple dark matter scenarios from ubiquitous stringy throats*, *Phys. Rev.* **D87** (2013), no. 6 063522, [[arXiv:1211.0250](#)].
- [76] J. Heeck and H. Zhang, *Exotic Charges, Multicomponent Dark Matter and Light Sterile*

- Neutrinos*, *JHEP* **05** (2013) 164, [[arXiv:1211.0538](#)].
- [77] A. Biswas, D. Majumdar, A. Sil, and P. Bhattacharjee, *Two Component Dark Matter : A Possible Explanation of 130 GeV  $\gamma$ - Ray Line from the Galactic Centre*, *JCAP* **1312** (2013) 049, [[arXiv:1301.3668](#)].
- [78] S. Bhattacharya, A. Drozd, B. Grzadkowski, and J. Wudka, *Two-Component Dark Matter*, *JHEP* **10** (2013) 158, [[arXiv:1309.2986](#)].
- [79] L. Bian, R. Ding, and B. Zhu, *Two Component Higgs-Portal Dark Matter*, *Phys. Lett.* **B728** (2014) 105–113, [[arXiv:1308.3851](#)].
- [80] L. Bian, T. Li, J. Shu, and X.-C. Wang, *Two component dark matter with multi-Higgs portals*, *JHEP* **03** (2015) 126, [[arXiv:1412.5443](#)].
- [81] S. Esch, M. Klasen, and C. E. Yaguna, *A minimal model for two-component dark matter*, *JHEP* **09** (2014) 108, [[arXiv:1406.0617](#)].
- [82] A. Karam and K. Tamvakis, *Dark matter and neutrino masses from a scale-invariant multi-Higgs portal*, *Phys. Rev.* **D92** (2015), no. 7 075010, [[arXiv:1508.03031](#)].
- [83] A. Karam and K. Tamvakis, *Dark Matter from a Classically Scale-Invariant  $SU(3)_X$* , *Phys. Rev.* **D94** (2016), no. 5 055004, [[arXiv:1607.01001](#)].
- [84] A. DiFranzo and G. Mohlabeng, *Multi-component Dark Matter through a Radiative Higgs Portal*, *JHEP* **01** (2017) 080, [[arXiv:1610.07606](#)].
- [85] S. Bhattacharya, P. Poulose, and P. Ghosh, *Multipartite Interacting Scalar Dark Matter in the light of updated LUX data*, *JCAP* **1704** (2017), no. 04 043, [[arXiv:1607.08461](#)].
- [86] A. Dutta Banik, M. Pandey, D. Majumdar, and A. Biswas, *Two component WIMP-FIMP dark matter model with singlet fermion, scalar and pseudo scalar*, *Eur. Phys. J.* **C77** (2017), no. 10 657, [[arXiv:1612.08621](#)].
- [87] M. Klasen, F. Lyonnet, and F. S. Queiroz, *NLO+NLL collider bounds, Dirac fermion and scalar dark matter in the  $B^?L$  model*, *Eur. Phys. J.* **C77** (2017), no. 5 348, [[arXiv:1607.06468](#)].
- [88] P. Ghosh, A. K. Saha, and A. Sil, *Study of Electroweak Vacuum Stability from Extended Higgs Portal of Dark Matter and Neutrinos*, *Phys. Rev.* **D97** (2018), no. 7 075034, [[arXiv:1706.04931](#)].
- [89] A. Ahmed, M. Duch, B. Grzadkowski, and M. Iglicki, *Multi-Component Dark Matter: the vector and fermion case*, [arXiv:1710.01853](#).

- [90] S. Bhattacharya, P. Ghosh, T. N. Maity, and T. S. Ray, *Mitigating Direct Detection Bounds in Non-minimal Higgs Portal Scalar Dark Matter Models*, *JHEP* **10** (2017) 088, [[arXiv:1706.04699](#)].
- [91] S. Bhattacharya, A. K. Saha, A. Sil, and J. Wudka, *Dark Matter as a remnant of SQCD Inflation*, *JHEP* **10** (2018) 124, [[arXiv:1805.03621](#)].
- [92] S. Bhattacharya, P. Ghosh, and N. Sahu, *Multipartite Dark Matter with Scalars, Fermions and signatures at LHC*, *JHEP* **02** (2019) 059, [[arXiv:1809.07474](#)].
- [93] M. Aoki and T. Toma, *Boosted Self-interacting Dark Matter in a Multi-component Dark Matter Model*, *JCAP* **1810** (2018), no. 10 020, [[arXiv:1806.09154](#)].
- [94] A. Dutta Banik, A. K. Saha, and A. Sil, *Scalar assisted singlet doublet fermion dark matter model and electroweak vacuum stability*, *Phys. Rev.* **D98** (2018), no. 7 075013, [[arXiv:1806.08080](#)].
- [95] B. Barman, S. Bhattacharya, and M. Zakeri, *Multipartite Dark Matter in  $SU(2)_N$  extension of Standard Model and signatures at the LHC*, *JCAP* **1809** (2018), no. 09 023, [[arXiv:1806.01129](#)].
- [96] S. Yaser Ayazi and A. Mohamadnejad, *Scale-Invariant Two Component Dark Matter*, *Eur. Phys. J.* **C79** (2019), no. 2 140, [[arXiv:1808.08706](#)].
- [97] A. Poulin and S. Godfrey, *Multi-component dark matter from a hidden gauged  $SU(3)$* , [[arXiv:1808.04901](#)].
- [98] S. Chakraborti and P. Poulou, *Interplay of Scalar and Fermionic Components in a Multi-component Dark Matter Scenario*, [[arXiv:1808.01979](#)].
- [99] S. Chakraborti, A. Dutta Banik, and R. Islam, *Probing Multicomponent Extension of Inert Doublet Model with a Vector Dark Matter*, [[arXiv:1810.05595](#)].
- [100] N. Bernal, D. Restrepo, C. Yaguna, and O. Zapata, *Two-component dark matter and a massless neutrino in a new  $B - L$  model*, [[arXiv:1808.03352](#)].
- [101] F. Elahi and S. Khatibi, *Multi-Component Dark Matter in a Non-Abelian Dark Sector*, [[arXiv:1902.04384](#)].
- [102] D. Borah, R. Roshan, and A. Sil, *Minimal Two-component Scalar Doublet Dark Matter with Radiative Neutrino Mass*, [[arXiv:1904.04837](#)].
- [103] S. Bhattacharya, N. Chakrabarty, R. Roshan, and A. Sil, *Multicomponent dark matter in extended  $U(1)_{B-L}$ : neutrino mass and high scale validity*, [[arXiv:1910.00612](#)].

- [104] D. Borah, S. Mahapatra, D. Nanda, and N. Sahu, *Inelastic Fermion Dark Matter Origin of XENON1T Excess with Muon  $(g - 2)$  and Light Neutrino Mass*, [arXiv:2007.10754](#).
- [105] P. Gondolo and G. Gelmini, *Cosmic abundances of stable particles: Improved analysis*, *Nucl. Phys.* **B360** (1991) 145–179.
- [106] N. G. Deshpande and E. Ma, *Pattern of Symmetry Breaking with Two Higgs Doublets*, *Phys. Rev.* **D18** (1978) 2574.
- [107] A. Dasgupta and D. Borah, *Scalar Dark Matter with Type II Seesaw*, *Nucl. Phys.* **B889** (2014) 637–649, [[arXiv:1404.5261](#)].
- [108] M. Cirelli, N. Fornengo, and A. Strumia, *Minimal dark matter*, *Nucl. Phys.* **B753** (2006) 178–194, [[hep-ph/0512090](#)].
- [109] R. Barbieri, L. J. Hall, and V. S. Rychkov, *Improved naturalness with a heavy Higgs: An Alternative road to LHC physics*, *Phys. Rev.* **D74** (2006) 015007, [[hep-ph/0603188](#)].
- [110] E. Ma, *Common origin of neutrino mass, dark matter, and baryogenesis*, *Mod. Phys. Lett.* **A21** (2006) 1777–1782, [[hep-ph/0605180](#)].
- [111] L. Lopez Honorez, E. Nezri, J. F. Oliver, and M. H. G. Tytgat, *The Inert Doublet Model: An Archetype for Dark Matter*, *JCAP* **0702** (2007) 028, [[hep-ph/0612275](#)].
- [112] E. M. Dolle and S. Su, *The Inert Dark Matter*, *Phys. Rev.* **D80** (2009) 055012, [[arXiv:0906.1609](#)].
- [113] L. Lopez Honorez and C. E. Yaguna, *The inert doublet model of dark matter revisited*, *JHEP* **09** (2010) 046, [[arXiv:1003.3125](#)].
- [114] L. Lopez Honorez and C. E. Yaguna, *A new viable region of the inert doublet model*, *JCAP* **1101** (2011) 002, [[arXiv:1011.1411](#)].
- [115] A. Goudelis, B. Herrmann, and O. Stal, *Dark matter in the Inert Doublet Model after the discovery of a Higgs-like boson at the LHC*, *JHEP* **09** (2013) 106, [[arXiv:1303.3010](#)].
- [116] A. Arhrib, Y.-L. S. Tsai, Q. Yuan, and T.-C. Yuan, *An Updated Analysis of Inert Higgs Doublet Model in light of the Recent Results from LUX, PLANCK, AMS-02 and LHC*, *JCAP* **1406** (2014) 030, [[arXiv:1310.0358](#)].
- [117] M. A. D??az, B. Koch, and S. Urrutia-Quiroga, *Constraints to Dark Matter from Inert Higgs Doublet Model*, *Adv. High Energy Phys.* **2016** (2016) 8278375, [[arXiv:1511.04429](#)].
- [118] A. Ahriche, A. Jueid, and S. Nasri, *Radiative neutrino mass and Majorana dark matter within an inert Higgs doublet model*, *Phys. Rev.* **D97** (2018), no. 9 095012,



- [arXiv:1710.03824].
- [119] D. Borah and A. Gupta, *New viable region of an inert Higgs doublet dark matter model with scotogenic extension*, *Phys. Rev.* **D96** (2017), no. 11 115012, [arXiv:1706.05034].
- [120] K. Griest and D. Seckel, *Three exceptions in the calculation of relic abundances*, *Phys. Rev.* **D43** (1991) 3191–3203.
- [121] V. Silveira and A. Zee, *SCALAR PHANTOMS*, *Phys. Lett.* **161B** (1985) 136–140.
- [122] J. McDonald, *Gauge singlet scalars as cold dark matter*, *Phys. Rev.* **D50** (1994) 3637–3649, [hep-ph/0702143].
- [123] C. P. Burgess, M. Pospelov, and T. ter Veldhuis, *The Minimal model of nonbaryonic dark matter: A Singlet scalar*, *Nucl. Phys.* **B619** (2001) 709–728, [hep-ph/0011335].
- [124] **GAMBIT** Collaboration, P. Athron et al., *Status of the scalar singlet dark matter model*, *Eur. Phys. J.* **C77** (2017), no. 8 568, [arXiv:1705.07931].
- [125] D. Borah, R. Roshan, and A. Sil, *Sub-TeV Singlet Scalar Dark Matter and Electroweak Vacuum Stability with Vector Like Fermions*, arXiv:2007.14904.
- [126] G. Belanger, F. Boudjema, A. Pukhov, and A. Semenov, *micrOMEGAs4.1: two dark matter candidates*, *Comput. Phys. Commun.* **192** (2015) 322–329, [arXiv:1407.6129].
- [127] A. Alloul, N. D. Christensen, C. Degrande, C. Duhr, and B. Fuks, *FeynRules 2.0 - A complete toolbox for tree-level phenomenology*, *Comput. Phys. Commun.* **185** (2014) 2250–2300, [arXiv:1310.1921].
- [128] A. Belyaev, N. D. Christensen, and A. Pukhov, *CalcHEP 3.4 for collider physics within and beyond the Standard Model*, *Comput. Phys. Commun.* **184** (2013) 1729–1769, [arXiv:1207.6082].
- [129] **XENON** Collaboration, E. Aprile et al., *First Dark Matter Search Results from the XENON1T Experiment*, *Phys. Rev. Lett.* **119** (2017), no. 18 181301, [arXiv:1705.06655].
- [130] E. Aprile et al., *Dark Matter Search Results from a One Tonne×Year Exposure of XENON1T*, arXiv:1805.12562.
- [131] **LUX** Collaboration, D. S. Akerib et al., *Results from a search for dark matter in the complete LUX exposure*, *Phys. Rev. Lett.* **118** (2017), no. 2 021303, [arXiv:1608.07648].
- [132] **PandaX-II** Collaboration, A. Tan et al., *Dark Matter Results from First 98.7 Days of Data from the PandaX-II Experiment*, *Phys. Rev. Lett.* **117** (2016), no. 12 121303, [arXiv:1607.07400].

- [133] **PandaX-II** Collaboration, X. Cui et al., *Dark Matter Results From 54-Ton-Day Exposure of PandaX-II Experiment*, *Phys. Rev. Lett.* **119** (2017), no. 18 181302, [[arXiv:1708.06917](#)].
- [134] J. Herrero-Garcia, A. Scaffidi, M. White, and A. G. Williams, *On the direct detection of multi-component dark matter: sensitivity studies and parameter estimation*, *JCAP* **11** (2017) 021, [[arXiv:1709.01945](#)].
- [135] J. Herrero-Garcia, A. Scaffidi, M. White, and A. G. Williams, *Time-dependent rate of multicomponent dark matter: Reproducing the DAMA/LIBRA phase-2 results*, *Phys. Rev. D* **98** (2018), no. 12 123007, [[arXiv:1804.08437](#)].
- [136] **KamLAND-Zen** Collaboration, A. Gando et al., *Search for Majorana Neutrinos near the Inverted Mass Hierarchy Region with KamLAND-Zen*, *Phys. Rev. Lett.* **117** (2016), no. 8 082503, [[arXiv:1605.02889](#)]. [Addendum: *Phys. Rev. Lett.* 117, no. 10, 109903 (2016)].
- [137] A. Vicente and C. E. Yaguna, *Probing the scotogenic model with lepton flavor violating processes*, *JHEP* **02** (2015) 144, [[arXiv:1412.2545](#)].
- [138] D. Borah, A. Dasgupta, K. Fujikura, S. K. Kang, and D. Mahanta, *Observable Gravitational Waves in Minimal Scotogenic Model*, [arXiv:2003.02276](#).